Seismic Assessment and Retrofit of Existing Multi-Column Bent Bridges

WA-RD 639.1

Research Report
January 2006

Washington State Department of Transportation

Washington State Transportation Commission
Research Office:
U.S. DOT - Federal Highway Administration

Seismic Assessment and Retrofit of Existing Multi-Column Bent Bridges

By Cole C. McDaniel, Assistant Professor
Department of Civil and Environmental Engineering
Washington State University
Pullman, WA 99164-2910

Submitted to:

The Washington State Department of Transportation

TECHNICAL REPORT STANDARD TITLE PAGE

1. REPORT NO.	2. GOVERNMENT ACCESSION NO.	3. RECIPIENTS CATALOG NO.
WA-RD 639.1		

4. TITLE AND SUBTITLE	5. REPORT DATE
Seismic Assessment and Retrofit of Existing Multi-Column Bent Bridges	February 2006
	6. PERFORMING ORGANIZATION CODE
7. AUTHOR(S)	8. PERFORMING ORGANIZATION REPORT NO.
Cole C. McDaniel	
9. PERFORMING ORGANIZATION NAME AND ADDRESS	10. WORK UNIT NO.
Washington State University Civil and Environmental Engineering Department PO Box 642910 Pullman, WA 99164-2910	11. CONTRACT OR GRANT NO. Agreement T2696, Task 10
12. SPONSORING AGENCY NAME AND ADDRESS	13. TYPE OF REPORT AND PERIOD COVERED
Research Office Washington State Department of Transportation Transportation Building, MS 47372 Olympia, WA 98504-7372 Kim Willoughby, Project Manager, 360-705-7978	Final Research Report
	14. SPONSORING AGENCY CODE

15. SUPPLEMENTARY NOTES

This study was conducted in cooperation with the U.S. Department of Transportation, Federal Highway Administration.

16. ABSTRACT

The main objective of this research was to assess the seismic vulnerability of typical pre-1975 WSDOT prestressed concrete multi-column bent bridges. Additional objectives included determining the influence of soil-structure-interaction on the bridge assessment and evaluating the effects of non-traditional retrofit schemes on the global response of the bridges. Overall this research highlighted the vulnerability of non-monolithic bridge decks and shear-dominated bridge columns in pre-1975 WSDOT prestressed concrete multi-column bent bridges as well as the importance of including soil-structure-interaction, calibrating the force/displacement characterization of the columns to experimental test data and detailed modeling of the bridges such as expansion joint/girder interaction. In the end, the seismic assessment of bridges is a cost/efficiency issue. Each bridge is different, therefore, investing in improved analyses up front will enable an efficient use of the limited funds for bridge improvement, resulting in a significant savings overall.

17. KEY WORDS	18. DISTRIBUTION STATEMENT
WSDOT, prestressed concrete, multi-column bent, bridges, seismic assessment, retrofit	No restrictions. This document is available to the public through the National Technical Information Service, Springfield, VA 22616

19. SECURITY CLASSIF. (of this report)	20. SECURITY CLASSIF. (of this page)	21. NO. OF PAGES	22. PRICE
None	None	63	

DISCLAIMER

The contents of this report reflect the view of the author, who is responsible for the facts and the accuracy of the data presented herein. The contents do not necessarily reflect the official views or policies of the Washington State Transportation Commission, Department of Transportation, or the Federal Highway Administration. This report does not constitute a standard, specification, or regulation.

TABLE OF CONTENTS

TABLE OF TABLES

TABLE OF FIGURES

Executive Summary

The Washington State Department of Transportation (WSDOT) has implemented retrofit schemes to improve the seismic performance of single column bent bridges throughout western Washington State. However, numerous multi-column bent bridges are also in need of seismic upgrade. Multi-column bent bridges targeted for retrofit include 2 to 5 column bents with simple precast prestressed concrete spans as well as continuous reinforced and prestressed concrete spans. The majority of these bridges were constructed in the 1950's and 1960's. The main objective of this research was to assess the seismic vulnerability of typical pre-1975 WSDOT prestressed concrete multi-column bent bridges. Additional objectives included determining the influence of soil-structure-interaction on the bridge assessment and evaluating the effects of non-traditional retrofit schemes on the global response of the bridges. WSDOT bridges 5/518, 5/826, and 5/227 were chosen in collaboration with WSDOT Bridge engineers for these studies. The bridges varied in span length, column aspect ratio, bridge deck design, and abutment and column foundation configurations.

Eight earthquake ground motions were used in this research: three 475-year return period ground motions (Mexico City, Mexico, 1985; Kobe , Japan, 1995; and Olympia, Washington, 1949) with peak ground accelerations (PGA's) of approximately 0.3g and spectral accelerations of approximately 0.7g for a structural period of 0.5 seconds ($S_{A(T=0.5s)}$, the three bridge fundamental periods ranged from 0.4-0.6 seconds); three 975-year return period ground motions (Mexico City, Mexico, 1985; Kobe , Japan, 1995; and Olympia, Washington, 1949) with PGA's of approximately 0.5g and $S_{A(T=0.5s)}$ of approximately 1.0g; and two predicted Cascadia Subduction-Zone (CSZ) earthquake ground motions (Moquegua, Peru, 2001; Llolleo, Chile, 1985) with PGA's of approximately 0.6g and $S_{A(T=0.5s)}$ of approximately 1.2g. These CSZ ground

motion spectral accelerations are similar to the 2003 United States Geological Survey (USGS) 2475-year return period spectral acceleration values for Seattle, WA, for structural periods equal to 0.5 seconds. All ground motions were modified appropriately to fit target acceleration response spectra for the Seattle area. As a point of comparison, the 2005 Earthquake Engineering Research Institute "Scenario for a Magnitude 6.7 Earthquake on the Seattle Fault" (EERI, 2005) predicted PGA's in Seattle exceeding 0.7g. In addition, the 2001 Nisqually, WA earthquake generated PGA's of approximately 0.3g (EERI, 2005).

The three pre-1975 WSDOT bridges were modeled as spine models with nonlinear column elements as well as expansion joints and soil-structure-interaction. The hysteretic behavior of the columns was calibrated to experimental test data for both the flexure-dominated (Stapleton, 2004) and shear-dominated pre-1975 WSDOT bridge columns (Jaradat, 1996). All three bridge models were subject to the eight ground motions to assess the bridge seismic vulnerability. The bridge deck design and the column aspect ratios greatly influenced the bridge response. For bridges 5/518 and 5/227, with non-monolithic decks and aspect ratios of 3.8 and 3 respectively, the column shear force/displacement demands approached the column shear force capacity envelope when subjected to the large CSZ ground motions; therefore, column failure is likely for these bridges in this case. For bridge 5/826, with a monolithic deck, a column aspect ratio of 4.2, and more column transverse reinforcement than the other two bridges, the column shear force/displacement demand did not approach the shear capacity envelope when subjected to the CSZ ground motions. Damage to the expansion joints was predicted for all three bridges under all the ground motions. Although moderate damage to the bridge columns (including extensive cracking and spalling of the cover concrete in the plastic hinge region) is likely,

column failure was not predicted in any of the bridge analyses using the 975-year return period ground motions.

The column footings were also assessed in each analysis; significant damage was not predicted. If the columns were retrofitted, for example by steel jacketing, resulting in an increase in the column shear force and displacement capacities and potentially an increase in the demands as well, the demands on the column footings may exceed the capacity of the footings. Therefore, further investigation of the foundations is necessary if column retrofit is implemented. Due to failure of prestressed concrete girders in one bridge during the 2001 Nisqually, WA earthquake, the girder demand/capacity ratios were also monitored closely, however, the demands did not exceed the capacities in any of the analyses. It is likely that significant dynamic amplification (which was not assessed in this research) occurred due to pounding of the girders against the girder stops, resulting in a torsional response of the girders, leading to large girder demands for that particular bridge. The girder damage in only one bridge during the 2001 Nisqually earthquake highlights the need for individual bridge assessment beyond simply identifying poor design details. This requires additional upfront costs for bridge analysis, but the result of logically prioritizing the bridges for retrofit will lead to significant savings overall.

The soil-structure-interaction study revealed that each bridge responded differently to variations in soil spring stiffnesses. When soil spring stiffnesses were changed, the maximum column displacements were noticeably different for all three bridges. Modeling the column footings with fixed boundary conditions and the abutments with rollers in the longitudinal direction resulted in inaccurate and often unconservative bridge seismic assessment, particularly the transverse response of the bridge, illustrating the need for including soil-structure-interaction to accurately model bridge seismic response.

Wrapping bridge columns with steel or composite jackets has already been proven effective for increasing bridge column force/displacement capacities. Therefore, non-traditional retrofitting methods were evaluated in this research, including friction dampers, viscous dampers, and transverse link beams. The goal of the retrofit schemes was to reduce the displacement demands on the bridges since the column force/displacement demand approached or exceeded the column shear capacity envelope in the pre-retrofit analyses. Retrofitting with friction and viscous dampers reduced the column displacement demand in all cases for the three bridges. Conversely, the transverse link beam retrofits increased column shear force/displacement demand beyond the column shear capacity envelope. Analytically, the optimum retrofit method for all three bridges was the viscous damper retrofit. The retrofits with viscous dampers were effective at reducing displacement and shear force demands in the columns. However, a cost analysis should be performed in order to choose which retrofit scheme to use for a given bridge.

Overall this research highlighted the vulnerability of non-monolithic bridge decks and shear-dominated bridge columns in pre-1975 WSDOT prestressed concrete multi-column bent bridges as well as the importance of including soil-structure-interaction, calibrating the force/displacement characterization of the columns to experimental test data and detailed modeling of the bridges such as expansion joint/girder interaction. In the end, the seismic assessment of bridges is a cost/efficiency issue. Each bridge is different, therefore, investing in improved analyses up front will enable an efficient use of the limited funds for bridge improvement, resulting in a significant savings overall.

Introduction

Background

Concrete bridge design inadequacies were revealed in the 1971 San Fernando Earthquake as well as the more recent 1989 Loma Prieta and 1994 Northridge earthquakes. Even though these earthquakes occurred in California, similar design issues are present in Washington State concrete bridges designed prior to 1975. The two main column inadequacies are light confinement reinforcement and short lap splices. Concrete columns were specified with No. 3 or No. 4 transverse reinforcing hoops spaced at 30.5 cm (12 in.) on center. To increase the capacity of the columns at large displacements, current standards require minimum transverse reinforcement of No. 3 spirals spaced at 10.2 cm (4 in.) on center (AASHTO, 2005). Inadequate lap splice lengths varying from $20d_b$ to $45d_b$ located in the plastic hinging regions of the bridge columns are not sufficient to resist lap splice failure. Current design methodology requires the lap splice to be a length of $60d_b$ and located at the mid-height of the column (AASHTO, 2005). Other pre-1975 bridge design inadequacies may include inadequate girder seat lengths at the abutments and bents, inadequately designed column and abutment foundation footings, inadequate number of girder stops, and poor joint detailing.

Bridges are lifeline structures in the transportation system. While new bridges are designed with improved seismic details, many existing bridges pose a threat of failure in a large earthquake. Currently, many pre-1975 single-column bent WSDOT bridges have been retrofitted, and many multi-column bent bridges have been slated for seismic retrofit. However, funds for bridge upgrades are limited. This research was funded to assess the need for retrofit of typical multi-column bent pre-stressed concrete bridges.

Objectives

The objectives of this study included:

- Determine the response of three typical WSDOT prestressed concrete multi-column bent bridges subject to eight earthquake ground motions
- Determine the capacity of the three bridges
- Determine the effects of soil-structure-interaction on the response of the bridges
- Assess seismic retrofit schemes

Seismic Activity in Western Washington State

Large magnitude earthquakes in the Pacific Northwest have occurred along the Cascadia Subduction Zone (CSZ) where the Juan de Fuca Plate, made of oceanic crust, subducts under the North American Plate, made of continental crust (see Figure 1). Recent geological evidence indicates that the potential exists for additional large earthquakes in the Pacific Northwest as a result of rupturing of the locked interface between the Juan de Fuca and the North American Plate. This rupture scenario would cause the longest earthquakes experienced in the Pacific Northwest in modern times (Gregor et al. 2002). Deep subduction zone earthquakes are a function of the size of the fault. Since the CSZ fault area is large, an earthquake larger than a moment magnitude of 9 could take place if the rupture occurs along the entire fault (PNSN, 2005).

The duration of strong ground motion at a site is related to the duration of rupture along a fault. Since the rupture velocity is generally a constant, the duration of rupture is then proportional to the size of the fault and hence proportional to earthquake magnitude. This correlation between duration and magnitude has been demonstrated by empirical studies (e.g.

Chang and Krinitzsky 1977, Dobry et al. 1978) and is supported by seismological models (e.g. Hanks and McGuire 1981). It is important to note that events with bilateral rupture (e.g. the 1989 Loma Prieta earthquake) will have significantly lower rupture times and hence will produce ground motions with shorter durations.

Another type of earthquake that could occur in the Puget Lowland results from crustal faults. Earthquakes of this mode can reach moment magnitudes of greater than 7 (PNSN, 2005). Active crustal faults exist under key cities including: Seattle, Tacoma, and Olympia, WA (PNSN, 2005). Currently, geologic mapping and surveying is being performed to determine how many additional crustal faults may be active in the Puget Lowlands.

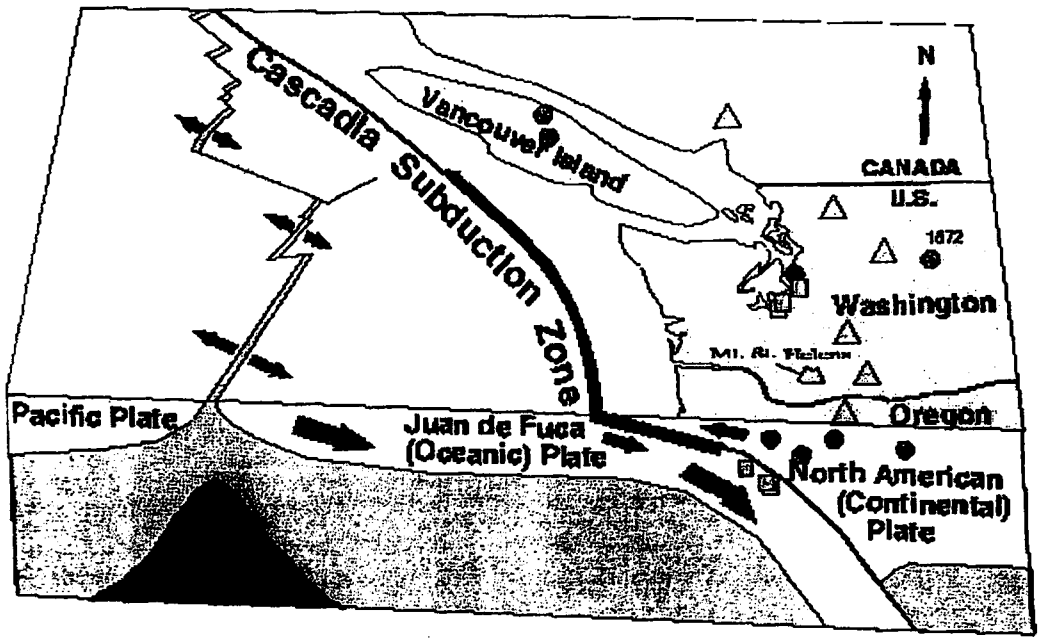

Figure 1 Cascadia Subduction Zone (from Ludwin, 2002)

Bridge Modeling

Three WSDOT bridges, 5/518, 5/826, and 5/227 were selected in collaboration with WSDOT engineers from a list of bridges slated for retrofit for study in this research. Constructed between the 1950's to 1970's, each bridge is characteristic of pre-1975 design

specifications. Ruaumoko3D (Carr, 2004) was used to model and analyze each bridge. Ruaumoko3D is a nonlinear time-history analysis package. The three bridges were analyzed as spine models including soil-structure-interaction.

Review of Previous Work

Concrete column failure is generally a result of deficiencies in flexure or shear strength. Insufficient lateral confinement as well as poor lap splice detailing can result in failure of a column in flexure. Insufficient transverse reinforcement can lead to shear failure, characterized by a steep degradation in strength once large enough post-yield displacements are reached. Short, lightly confined columns are especially susceptible to shear failure. The current seismic retrofit strategy for bridge substructures in the Pacific Northwest is to encase columns in steel jackets, thereby, improving the lateral confinement and ensuring a ductile flexural response rather than limited flexural ductility or a brittle shear mechanism. In the past, conventional retrofit strategies for single and multi-column bridge bents have been investigated, including work at Washington State University experimentally by Mealy (1997) and analytically by Zhang (1997). Professor M. J. Nigel Priestley and Frieder Seible (Priestley et.al. 1996) also have performed experimental and analytical studies on the retrofit of existing multi-column bridge bents including the development of the steel jacket concept. Conventional retrofit strategies aim to increase the bridge capacity.

Another approach is to reduce the bridge demands through passive protective systems such as friction and viscous dampers. Friction dampers have the distinction of being independent of excitation velocity and are limited by internal forces. Viscous dampers are dependant upon velocity and are not limited by forces (Filiatrault, 2002). Friction dampers are usually designed to only slip during large event earthquakes. Energy is dissipated when the

friction surfaces move along the slip plane. Viscous dampers respond out-of-phase with a structure's maximum seismic response. As a result, the damper experiences higher forces at lower structural demand, and lower forces at higher structural demand (Filiatrault, 2002). Large displacements are required in order for the dampers to be most effective. A thorough literature review on friction and viscous dampers was presented by Vader (2004). In this work, the history, the results of research performed, as well as the advantages and disadvantages of dampers were presented. The reader is referred to this work for more information on friction and viscous dampers.

An additional method for retrofitting columns is adding a transverse link beam. The location of the link beam is determined by whether the force or displacement capacity needs to be increased (Priestly et al., 1996). Placing the link beam at the column mid-height reduces column displacements most effectively. Placing the link at a higher location reduces the shear demand in the cap beam most effectively. However, shear demand in the columns will increase as the stiffness of the bent increases. Thus, adequate column shear capacity should be checked. If plastic hinging is forced to occur in the columns near the location of the link beam, then large plastic rotations can be expected.

Research Approach - Hysteresis Model

Determining the appropriate force-displacement characterization for the columns in the modeled bridges was a key aspect in obtaining accurate results. Failure in lightly confined concrete bridge columns with inadequate lap splice length can be a function of flexure, shear, and/or lap splice slippage. Experimental work performed by Jaradat (1996) and Stapleton (2004) was used to calibrate the force-displacement response for the columns in bridges 5/227, 5/518, and 5/826. Both experimental programs focused on pre-1975 WSDOT bridge columns; Jaradat

(1996) tested shear-dominated columns and Stapleton (2004) tested flexure-dominated columns. Calibrating the bridge 5/518 column force-displacement response is presented here.

Calibrating Bridge 5/518 to Stapleton (2004)

In this research, pushover analyses were performed for Stapleton's experimentally tested column to determine if the force-displacement characterization could properly modeled analytically. Because the tested columns were scaled to a factor of 1:2, a pushover analyses were also performed on full scale prototype columns of Stapleton's research to calibrate the columns for bridge 5/518. Figure 2 shows the results from one of Stapleton's full-scale prototype column. The analytical prediction of the elastic portion of the force-displacement curve matched the experimental data closely. The solid curve with strength degradation starting at about 3.5 in. (9 cm) was based on curvature ductility values determined from a flexural moment-curvature analysis (Priestley et al., 1996). The scaled experimental results showed that strength degradation occurred at curvature ductility larger than the analytical flexural capacity model predicted. This is expected since the moment curvature analysis prediction is considered conservative (Priestley et al., 1996). The bold solid curve with strength degradation beginning at about 1.8 in. (4.6 cm) was based on curvature ductility values determined from lap splice moment-curvature relationships (Priestley et al., 1996). This prediction was very conservative and significantly under-predicted the column capacity since the prediction was based on a lap splice length of $20d_b$ while the lap splice length in Stapleton's column was $35d_b$. This supports the view that strength degradation in the experimental force-displacement curve did not result from lap splice failure. The shear capacity envelope proposed by Kowalsky and Priestley (2000) is represented by the dashed line in the corners of the plot. The shear capacity envelope was not

a controlling failure mode for this column. Therefore, the strength degradation based on moment curvature analysis was used to conservatively model the column force/displacement response. The columns for bridges 5/826 and 5/227 were also calibrated using the above approach.

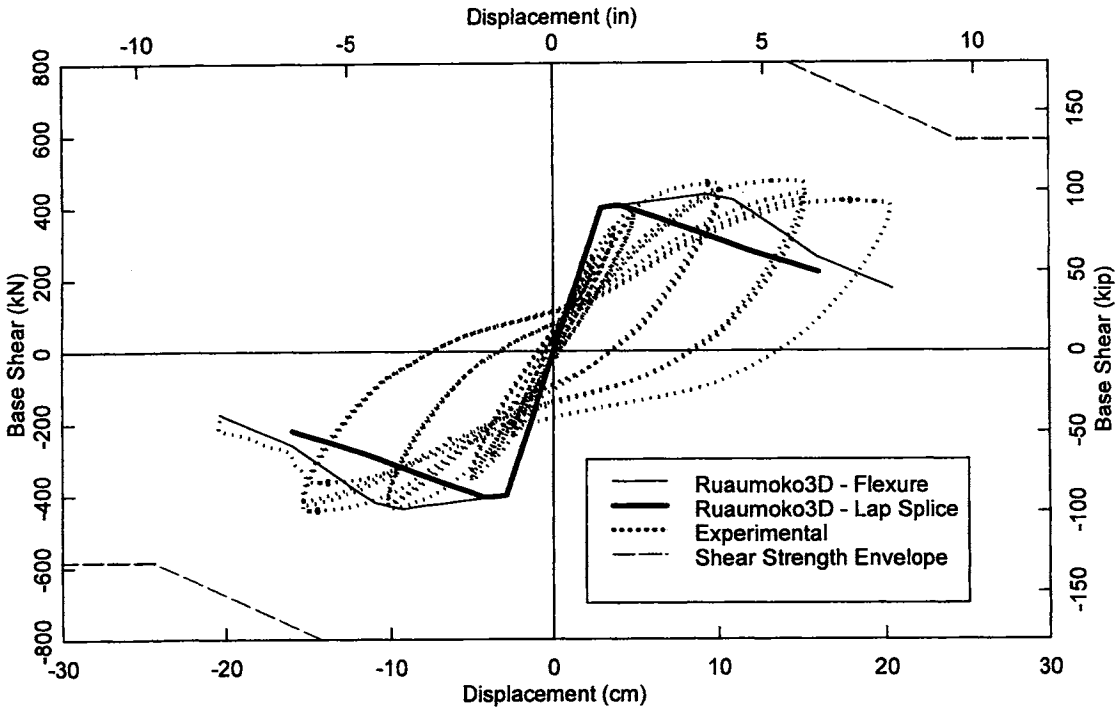

Figure 2 Stapleton Prototype Force-Displacement

Research Approach – Bridge Modeling

Seismic Excitations

For this research, the eight earthquake acceleration records used were one from the Moquegua, Peru (2001) earthquake; one from the Llolleo, Chile (1985) earthquake; two from the Mexico City, Mexico (1985) earthquake; two from the Kobe, Japan (1995) earthquake; and two

from the Olympia, Washington (1949) earthquake. Depending upon location in the Puget Sound, the Moquegua, Peru and Llolleo, Chile earthquakes had a 2475 to 4975-year return period, while the other six earthquakes had a 475 year and a 975-year return period. The Moquegua, Peru, Llolleo, Chile, and Mexico City, Mexico ground motions are from long-duration earthquakes, while the other ground motions are short-duration events. Additionally, the Moquegua, Peru and Llolleo, Chile ground motions are from subduction-zone earthquakes. The Moquegua, Peru and Llolleo, Chile ground motions were modified at Washington State University under the direction of Dr. Adrian Rodriguez-Marek (Stapleton, 2004). The other six ground motions were provided by WSDOT, which were specifically created by PanGEO Inc. for the Aurora Avenue bridge retrofit. Background on the provided design ground motions can be found at http://pangeoinc.com:

> "PanGEO provided design ground motions using both probabilistic and deterministic approaches. The current WSDOT (500-year return interval), CalTrans (1000 year) and UBC (1000 year) criteria, as well as the 2000 IBC (2,500 year) design requirements were utilized in the probabilistic approach to develop design ground motions. Geotechnical and topographical factors that could impact the design ground motions were considered in our evaluation, including the depth to the bedrock, Seattle Fault, existing fill adjacent to columns, soil liquefaction, and non-linear dynamic soil properties." (PanGEO Inc., 2005).

The vertical component of each ground motion was the N-S component scaled by 2/3. The N-S and E-W components correspond to the transverse and longitudinal axes of the bridges, respectively. Three attenuation relationships were reviewed for this study. The Atkinson and Boore (2003) relationship was chosen as the basis for creating the target spectrum for this

research since it includes a near-source saturation term, more precise soil classification than the other attenuation relationships, and is based on a larger database of ground motions than the other attenuation relationships, including ground motions with moment magnitudes of 8.0 and greater.

The attenuation relationship was generated for a soil site (NEHRP Soil type "D") based on a moment magnitude 8.5 event. The depth of the rupture is approximately 60km and the nearest distance to the fault is approximately 65km. The earthquake is the result of interface slipping. Depth of the rupture and distance to the fault were estimated for the Seattle, Washington. Ground motions were modified to fit the target 5% damped acceleration spectrum using the program RSPMATCH (Abrahamson 1998). This program alters the frequency content of a ground motion by adding pulses of motion in the form of tapered cosine waves. The end result is a ground motion of the desired frequency content and PGA.

Figure 3 shows the target acceleration spectrum produced by using the attenuation relationship from Atkinson and Boore (2003), the acceleration spectra of the original East-West ground motions of the Moquegua, Peru Earthquake, and the acceleration spectra of the modified Moquegua, Peru Earthquake ground motions after being modified in RSPMATCH (Abrahamson 1998) to match the target acceleration spectrum defined by Atkinson and Boore (2003). Figure 4 shows that the main characteristics of the ground motion were preserved after manipulation. Figures 5 through 12 show the N-S and E-W time-history excitations.

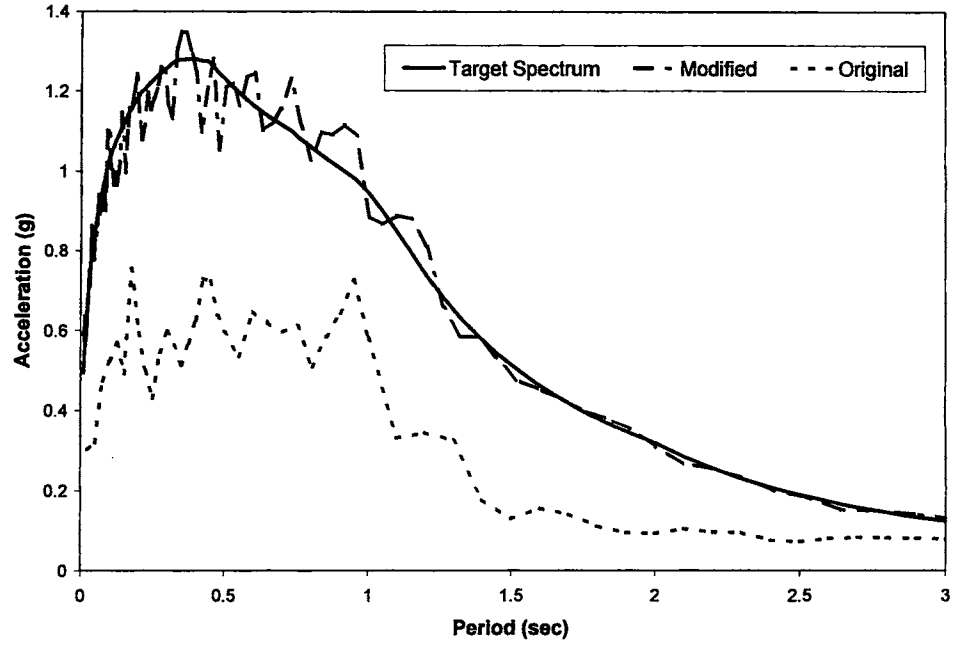

Figure 3 Moquegua, Peru Ground Motion (E-W) Spectral Acceleration

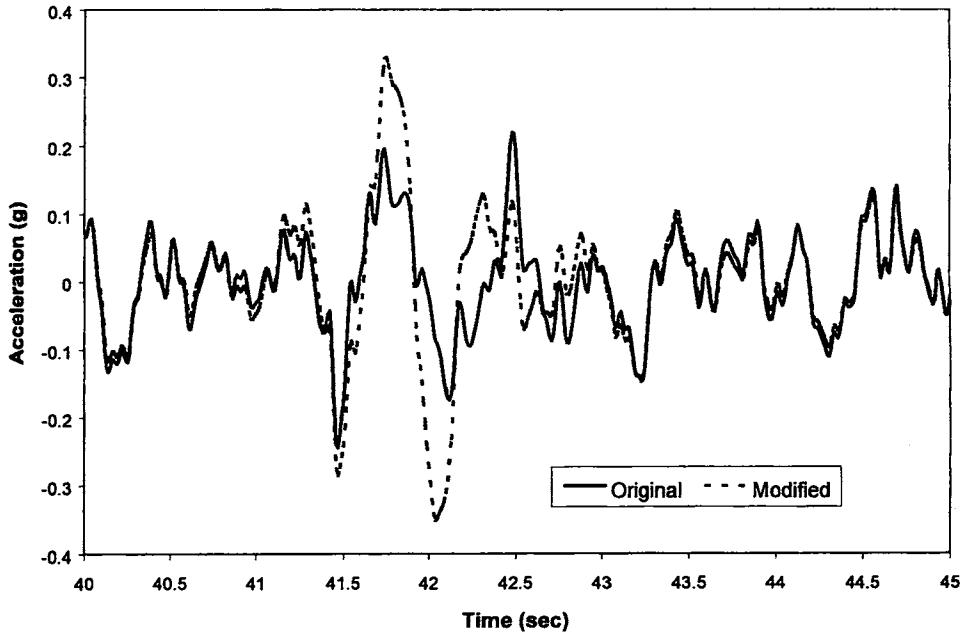

Figure 4 Modified and Original Moquegua, Peru Ground Motion (E-W) Time History

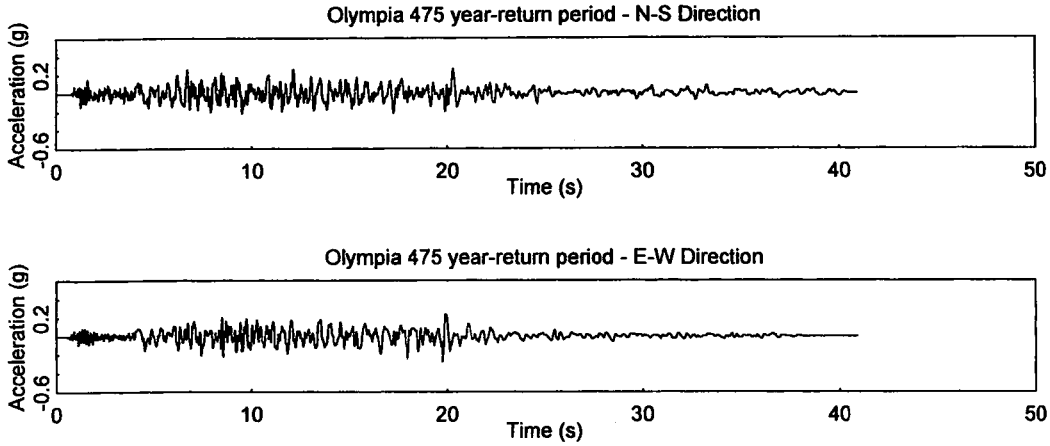

Figure 5 Time Histories for Olympia 475

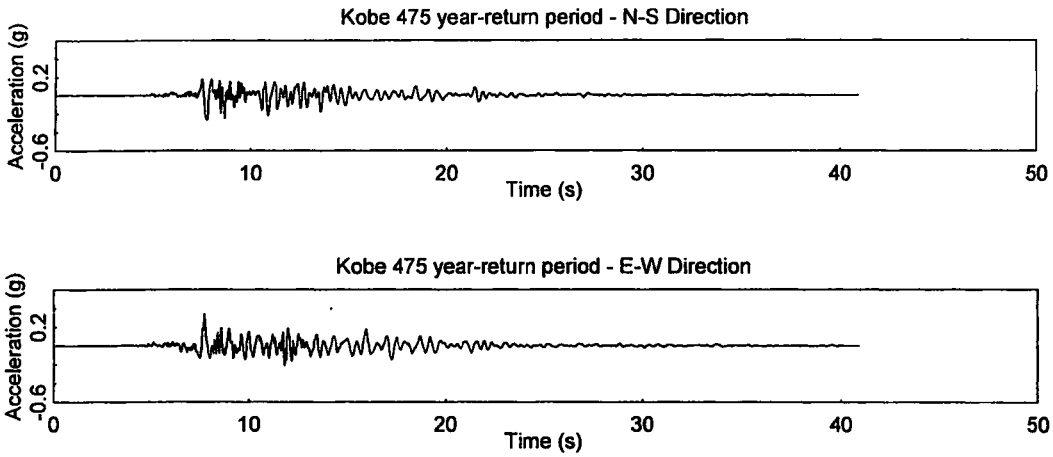

Figure 6 Time Histories for Kobe 475

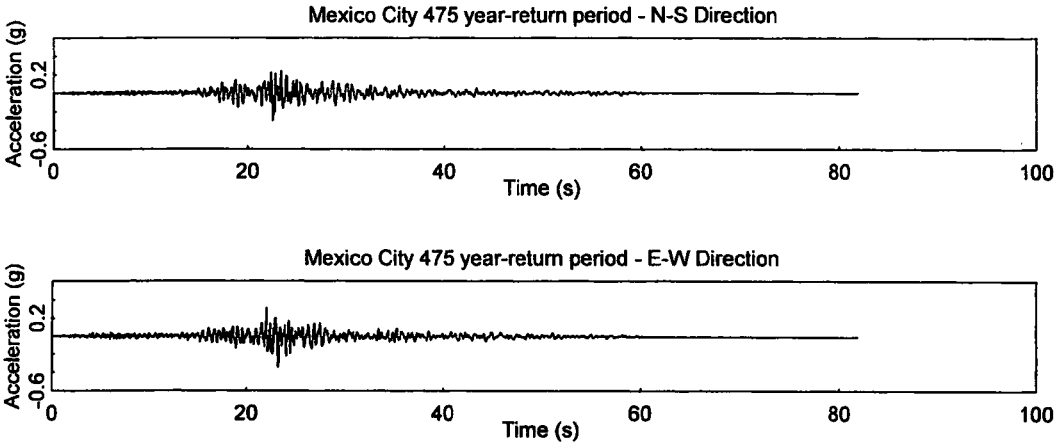

Figure 7 Time Histories for Mexico City 475

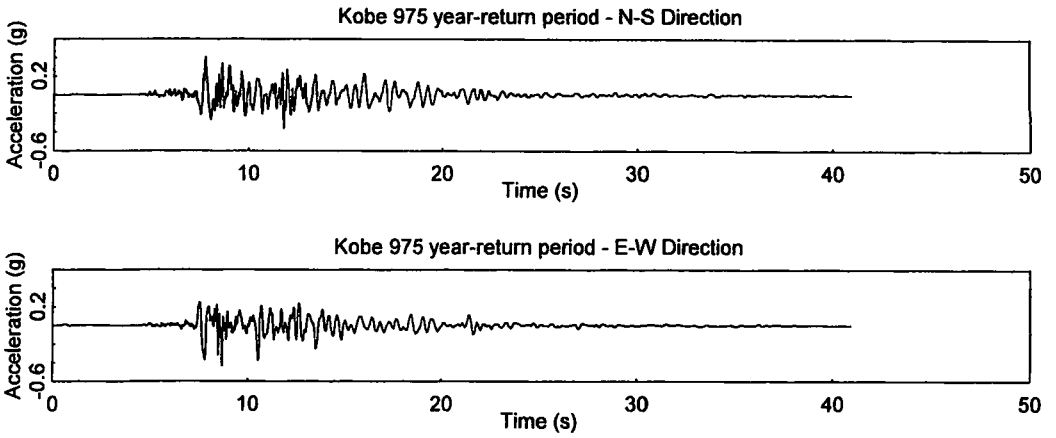

Figure 8 Time Histories for Kobe 975

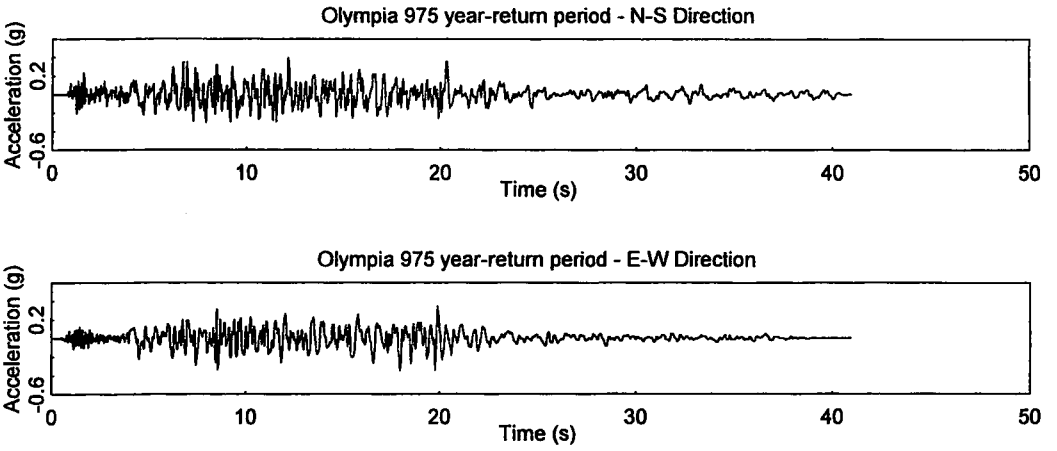

Figure 9 Time Histories for Olympia 975

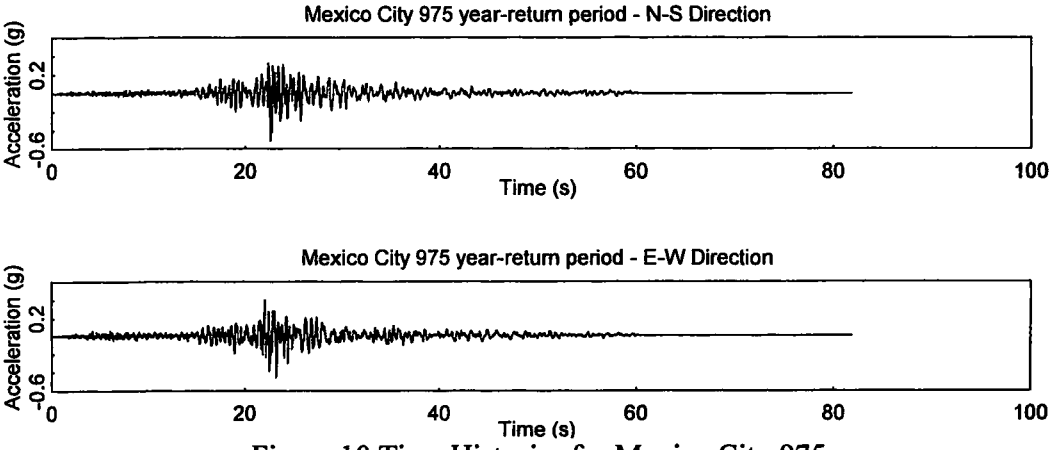

Figure 10 Time Histories for Mexico City 975

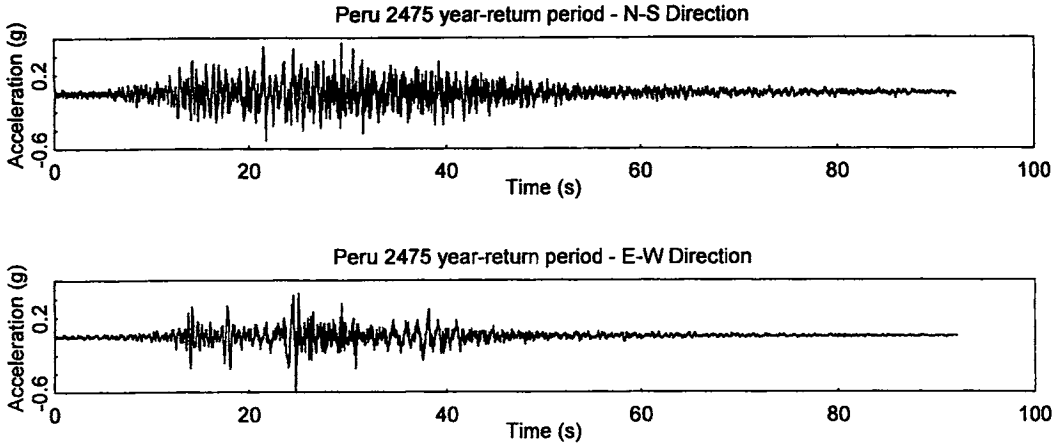

Figure 11 Time Histories for Peru 2475

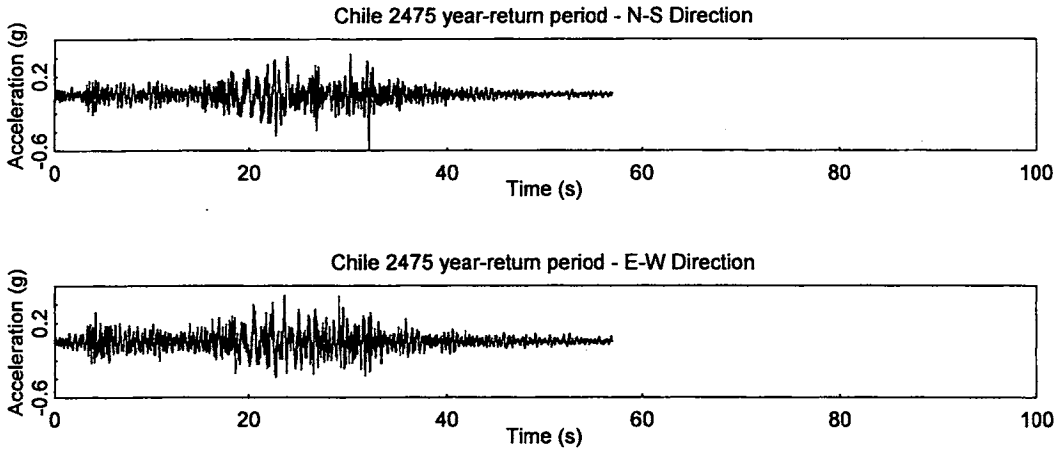

Figure 12 Time Histories for Chile 2475

WSDOT Bridges 5/518, 5/227, and 5/826

Introduction

Bridge 5/518 is an overpass located along 178th Street in King County, Washington. In 1964, the bridge was built to service traffic on 178th Street over the Interstate 5 Highway. Bridge 5/227 is an overpass located along Chamber Way in Lewis County, Washington. In 1958, the bridge was built to service traffic on Chamber Way over the Interstate 5 Highway. Bridge 5/826

is an overpass located along Smith Road in Whatcom County, Washington. In 1972, the bridge was built to service traffic on Smith Road over the Interstate 5 Highway. Typical WSDOT design standards prior to 1975 were used in the design of the three bridges.

Description of Bridges

Elevation and plan views of bridges 5/518, 5/227, and 5/826 are shown below in figures 13 through 18.

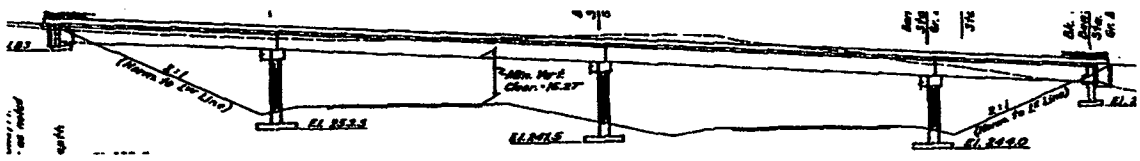

Figure 13 Elevation View for Bridge 5/518

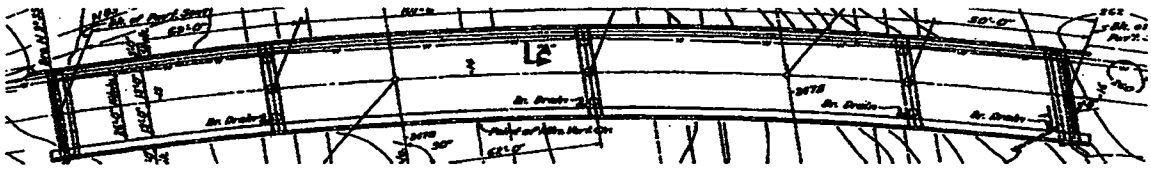

Figure 14 Plan View of Bridge 5/518

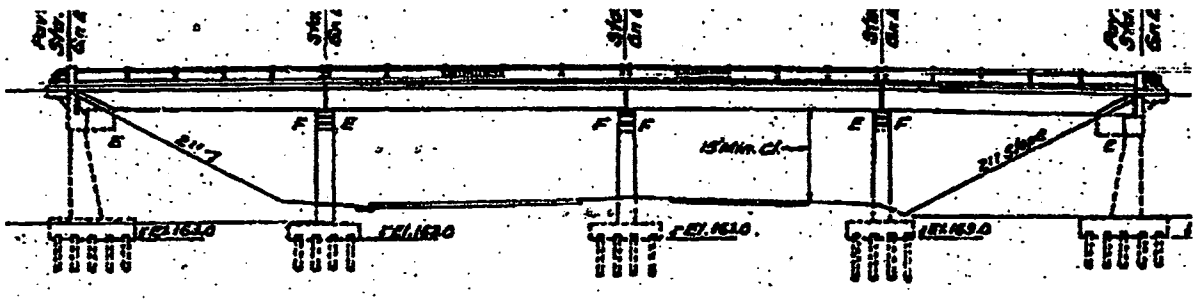

Figure 15 Elevation View of Bridge 5/227

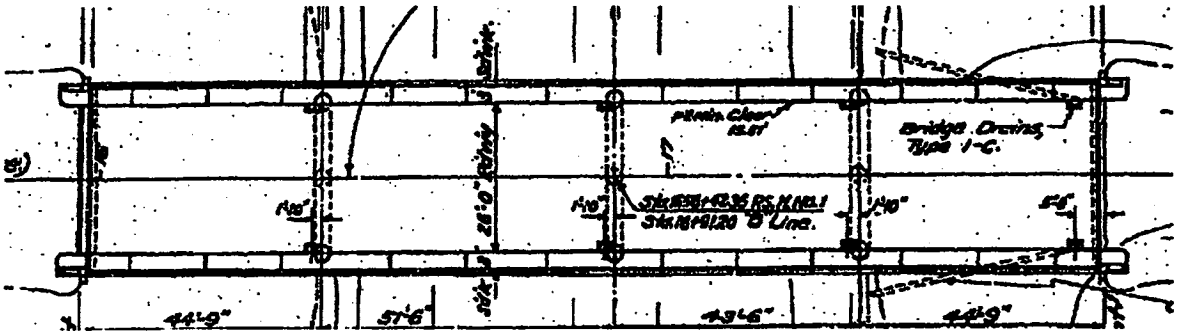

Figure 16 Plan View of Bridge 5/227

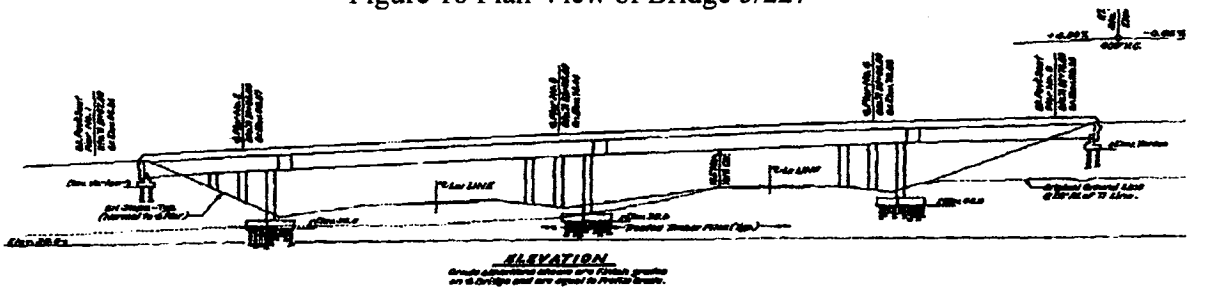

Figure 17 Elevation View of Bridge 5/826

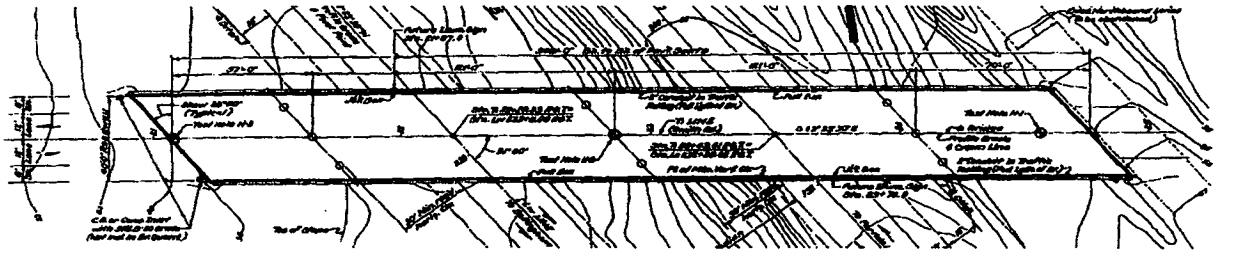

Figure 18 Plan View of Bridge 5/826

The bridged decks are composed of pre-cast, pre- and post-tensioned standard WSDOT I-girders. For bridges 5/518 and 5/227, the I-girders rest upon elastomeric bearing pads located on top of the column crossbeams and bridge deck abutment seats. For bridge 5/826, these bearing pads were only located at the abutment seats. The elastomeric bearing pad lies between asphaltic girder stops located between each neighboring girder at the crossbeam that provides transverse translational restraint for the bridge deck. The deck for bridges 5/518 and 5/227 was non-monolithically constructed. Between each span is a 1 in. (2.5 cm) expansion joint. The deck for bridge 5/826 was monolithically constructed.

For bridge 5/518, the height of the columns at the west bent and center bent are approximately 24 ft (7.3 m). The column heights at the east bent are approximately 21.5 ft (6.6 m). Each column has a cross-sectional diameter of 36 in. (0.91 m). Eleven evenly spaced No. 11 bars provide the longitudinal reinforcement within each column, ρ_L= 1.68%. Each column has a lap splice length of $35d_b$. Transverse reinforcement is provided by No. 3 bars spaced at 12 in. (30.5 cm) on center, ρ_t= 0.118%. Supporting each column is a spread footing.

For bridge 5/227, the height of the columns at the west bent outer columns are 19.4 ft (5.91 m) while the inner west bent column is about 19 ft (5.79 m). The center bent outer columns are 19.6 ft (5.97 m) and the inner center bent column is approximately 19 ft (5.79 m). The column heights at the east bent for the outer columns are 17.6 ft (5.36 m) and the inner column height is about 18 ft (5.49 m). Each column has a cross-sectional diameter of 36 in. (0.91 m). Eight evenly spaced No. 10 bars provide the longitudinal reinforcement within each column, ρ_L= 0.998%. Each column has a lap splice length of $20d_b$. Transverse reinforcement is provided by No. 3 bars spaced at 12 in. (30.5 cm) on center, ρ_t= 0.118%. Supporting each column is a spread footing with concrete piles.

For bridge 5/826, the height of the columns at the west bent are 25 ft (7.6 m), the center bent column heights are approximately 28 ft (8.5 m), and the column heights at the east bent are approximately 26.5 ft (8.1 m). Each column has a cross-sectional diameter of 36 in. (0.91 m). Seventeen evenly spaced No. 11 bars provide the longitudinal reinforcement within each column, ρ_L= 2.61%. Each column has a lap splice length of $45d_b$,. Transverse reinforcement is provided by No. 4 bars spaced at 6 inches on center, ρ_t= 0.43%. This is significantly more transverse confinement than in bridges 5/518 and 5/227. Supporting each column is a spread footing with treated timber piles.

For bridge 5/518, the east abutment is similar to the west abutment, except for two sub-ground columns with spread footings. For bridge 5/227, two sub-ground columns with spread footings and concrete piles are located under the west and east abutments. Each sub-ground footing has 20 concrete piles. For bridge 5/826, the western abutment has two rows of ten treated timber piles running in the transverse direction. The eastern abutment consists of two rows of eleven treated timber piles.

The footings and abutment walls were constructed with WSDOT Class B mix concrete providing a compressive strength of f'c = 3 ksi (20.7 kPa). The rest of the cast-in-place concrete in the bridges is WSDOT Class A concrete mix with a compressive strength of f'c = 4 ksi (27.6 MPa). The reinforcing steel is Grade 40 with a theoretical yield strength of fy = 40 ksi (276 MPa).

Structural Models

The bridge 5/518, 5/227, and 5/826 models are shown in figures 19 and 20. For bridges 5/518 and 5/227, the internal moments about the local z and x axes were released at the girder ends to model a simply supported boundary condition at the abutments and bents. The internal moments at the girder ends were released at only the abutments for bridge 5/826.

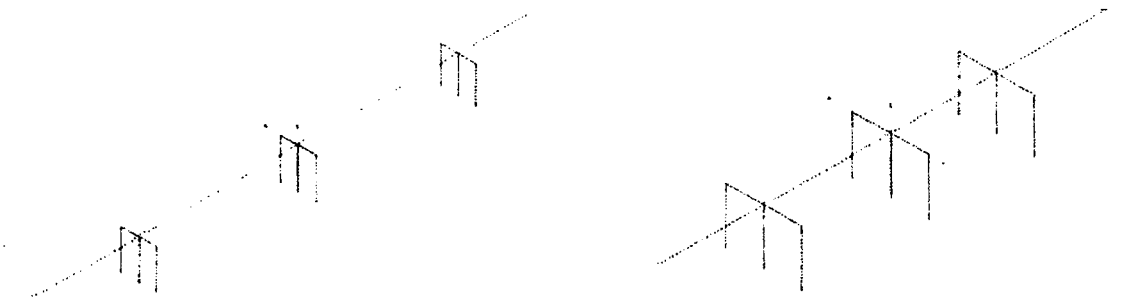

(a) (b)

Figure 19 (a) Bridge 5/518 Model, (b) Bridge 5/227 Model

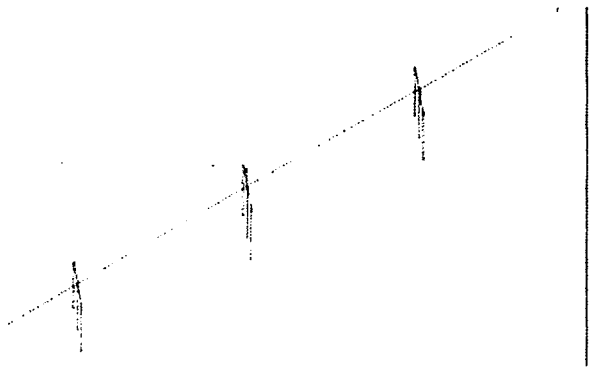

Figure 20 Bridge 5/826 Spine Model

For bridges 5/518 and 5/227, linear springs representing bearing pads connected each girder to the abutments and bents. For bridge 5/826, these springs existed at only the abutments. Expansion joints existed at all bents and abutments for bridges 5/518 and 5/227. For bridge 5/826, expansion joints existed only at the abutments. The expansion joints were modeled with nonlinear multi-spring members. The multi-spring member worked by offsetting nonlinear springs at discrete distances along the transverse direction of the bridge model. A total height (h), which was the transverse width of the bridge deck, was specified. Each of these offset springs had assigned stiffnesses for the translational and rotational degrees of freedom.

Each bridge column was modeled as a nonlinear beam-column element. The moment of inertia of the column was reduced to account for cracking. The reduction is a function of the axial load on a column and the longitudinal reinforcing ratio and was calibrated to experimental data. At the bottom and top of the columns, short rigid frame members existed to replicate the stiff foundation and crossbeam, respectively. Plastic hinges were modeled at the top and bottom of the columns in both directions. The Modified Takeda Hysteresis rule was implemented to describe the post-yield behavior of the columns.

Abutment and Column Footing Soil Springs

Abutment and footing soil stiffness springs were varied to study the effects on the response of the bridges. To determine the abutment and column footing soil spring stiffness values, the methods proposed by Lam et al. (1986) and CALTRANS (2004) were used. For bridges 5/826 and 5/227 with stiffness contributions from piles, the computer program LPILE4.0 (2000) was used. Pile group effects have been considered based on pile spacing for each footing. Reduction was based on recommendations given by WSDOT (2005).

The demand on the bridge footings did not exceed the design capacity, so yielding was not considered in the modeling of the column footings or abutment footings. The soil modulus of elasticity (E_s) was modified to vary the soil spring stiffness values. The soil modulus of elasticity was only varied for the spread footing contribution of the bridge models. This was due to limited information regarding the soil type along the length of the piles and the high variability of soil conditions along the length of the piles. For all analyses, Poisson's ratio was set at 0.45, a common value for saturated soils (Bowles, 1995). Nonlinear behavior of soil was simplified into a secant stiffness relationship.

A secant spring stiffness was implemented to account for the longitudinal abutment backwall stiffness also. The secant stiffness was based upon the procedure presented in chapter 7 of the CALTRANS seismic design criteria (CALTRANS, 2004). Because all abutments in this research are non-monolithic, only the stiffness from the abutment structure was enacted until the gap between the bridge deck and abutment back wall was closed. The longitudinal stiffness at each abutment was divided in half to address the passive resistance of the mobilized soil. Due to lack of or very short wingwalls, the contribution to the transverse resistance was ignored. Figure 21 is a diagram of the three stiffness components of the abutments. The contribution

from the abutment backwall, spread footing, and piles were lumped into one discrete spring for the spine models. At the column footings, the contributions from spread footings and piles were similarly lumped at one discrete location per footing.

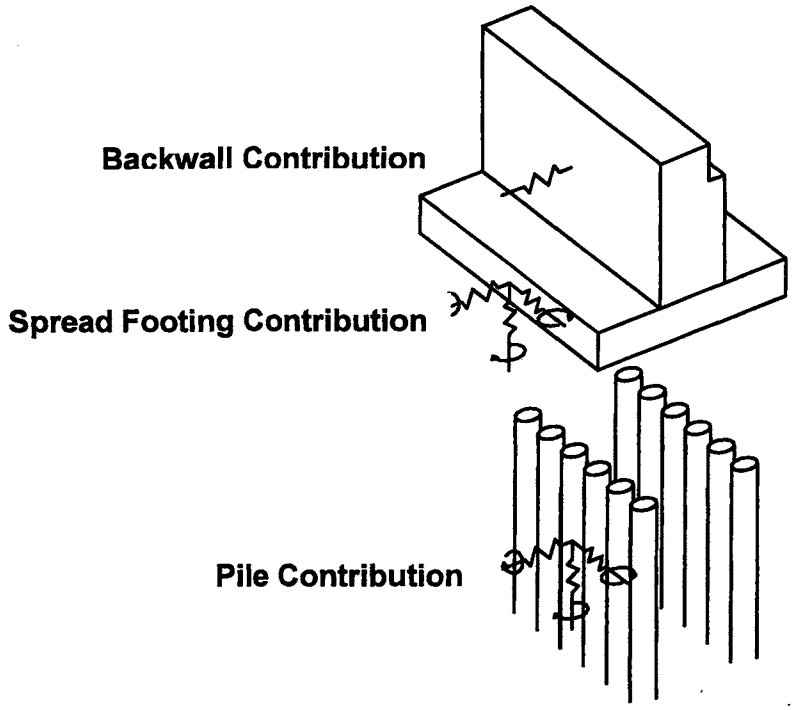

Figure 21 Abutment Soil Spring Diagram

Bridge Soil Spring Stiffness Values

Tables 1 through 3 show the total soil spring stiffness values for all contributions applied at the abutments and column footings for bridges 5/518, 5/826, and 5/227, respectively.

Table 1 Bridge 5/518 Soil Spring Stiffnesses

Bridge 5/518	Es (ksf)	Es (MPa)	K_{11} (Global X) k/ft	K_{22} (Global Y) k/ft	K_{33} (Global Z) k/ft	K_{44} (Global X) k-ft/rad	K_{55} (Global Y) k-ft/rad	K_{66} (Global Z) k-ft/rad
West Abut	1,000	47.9	19,940	26,038	22,475	410,822	3,262,975	2,193,510
	2,000	95.8	39,880	45,978	44,950	821,644	6,525,212	4,387,019
	6,000	287.3	119,570	125,669	134,782	2,464,195	19,575,635	13,161,795
	18,000	861.8	358,780	364,878	404,415	7,392,585	58,727,643	39,486,124
West Bent	1,000	47.9	15,829	15,829	16,377	747,150	458,764	819,431
	2,000	95.8	31,657	31,657	32,685	1,494,301	917,527	1,638,125
	6,000	287.3	94,903	94,903	98,055	4,483,640	2,751,844	4,914,376
	18,000	861.8	284,776	284,776	294,232	13,450,920	8,254,795	14,743,129
Center Bent	1,000	47.9	16,377	16,377	17,199	804,680	583,412	780,341
	2,000	95.8	32,685	32,685	34,398	1,609,360	1,166,823	1,560,681
	6,000	287.3	98,055	98,055	103,194	4,828,081	3,500,470	4,682,044
	18,000	861.8	294,164	294,164	309,581	14,483,507	10,502,147	14,046,132
East Bent	1,000	47.9	15,212	15,212	15,760	696,259	348,129	737,562
	2,000	95.8	30,424	30,424	31,589	1,392,517	696,259	1,475,124
	6,000	287.3	91,202	91,202	94,766	4,178,289	2,088,038	4,424,635
	18,000	861.8	273,676	273,676	284,297	12,534,130	6,264,115	13,273,905
East Abut	1,000	47.9	56,393	62,423	58,929	1,644,026	4,495,441	3,426,713
	2,000	95.8	112,718	118,817	117,789	3,287,314	8,991,619	6,853,427
	6,000	287.3	338,223	344,253	353,435	9,862,680	26,974,121	20,560,281
	18,000	861.8	1,014,602	1,020,632	1,060,237	29,588,041	80,923,099	61,681,580

Table 2 Bridge 5/826 Soil Spring Stiffnesses

Bridge 5/826	Es (ksf)	Es (MPa)	K_{11} (Global X) k/ft	K_{22} (Global Y) k/ft	K_{33} (Global Z) k/ft	K_{44} (Global X) k-ft/rad	K_{55} (Global Y) k-ft/rad	K_{66} (Global Z) k-ft/rad
West Abut	100	4.8	53,515	60,162	156,435	8,565	96,684	73,113
	1,000	47.9	74,278	80,924	181,514	57,079	938,611	731,059
	2,000	95.8	97,369	103,948	209,334	111,074	1,874,070	1,462,117
	6,000	287.3	189,668	196,246	320,682	326,986	5,615,838	4,386,420
	18,000	861.8	466,565	473,143	654,794	974,722	16,841,347	13,159,330
West Bent	100	4.8	15,691	15,691	45,087	11,786	11,786	15,897
	1,000	47.9	33,644	33,644	63,588	113,609	113,609	158,970
	2,000	95.8	53,584	53,584	84,076	226,739	226,739	318,009
	6,000	287.3	133,412	133,412	166,234	679,188	679,188	953,960
	18,000	861.8	372,758	372,758	412,707	2,036,604	2,036,604	2,861,880
Center Bent	100	4.8	16,925	16,925	51,254	11,854	11,854	15,897
	1,000	47.9	34,878	34,878	69,687	113,678	113,678	158,970
	2,000	95.8	54,817	54,817	90,243	226,807	226,807	318,009
	6,000	287.3	134,577	134,577	172,401	679,256	679,256	953,960
	18,000	861.8	373,923	373,923	418,874	2,036,672	2,036,672	2,861,880
East Bent	100	4.8	3,221	3,221	45,087	11,580	11,580	15,897
	1,000	47.9	21,173	21,173	63,588	113,404	113,404	158,970
	2,000	95.8	41,113	41,113	84,076	226,533	226,533	318,009
	6,000	287.3	120,941	120,941	166,234	678,982	678,982	953,960
	18,000	861.8	360,287	360,287	412,707	2,036,398	2,036,398	2,861,880
East Abut	100	4.8	64,410	71,057	171,784	8,908	97,095	73,113
	1,000	47.9	85,173	91,819	196,863	57,490	938,954	731,059
	2,000	95.8	108,264	114,911	224,683	111,485	1,874,413	1,462,117
	6,000	287.3	200,563	207,210	336,099	327,397	5,616,249	4,386,420
	18,000	861.8	477,460	484,106	670,143	975,133	16,841,758	13,159,330

Table 3 Bridge 5/227 Soil Spring Stiffnesses

Bridge 5/227	Es (ksf)	Es (MPa)	K_{11} (Global X) k/ft	K_{11} (Global X) k/ft	K_{22} (Global Y) k/ft	K_{33} (Global Z) k-ft/rad	K_{44} (Global X) k-ft/rad	K_{55} (Global Y) k-ft/rad
West Abut	5	0.24	78,732	84,830	319,928	1,279,027	1,279,644	2,878
	50	2.4	81,609	87,639	322,875	1,294,239	1,300,132	28,985
	100	4.8	84,830	90,860	326,164	1,311,095	1,322,881	57,901
	1,000	47.9	142,457	148,007	385,435	1,614,578	1,732,367	579,077
	2,000	95.8	206,525	211,595	451,284	1,951,774	2,187,352	1,158,223
	6,000	287.3	462,727	465,811	714,613	3,300,693	4,007,427	3,474,601
	18,000	861.8	1,231,405	1,228,458	1,504,601	7,347,451	9,467,515	10,423,736
West Bent	5	0.24	19,803	19,803	93,327	49,610	49,473	411
	50	2.4	20,625	20,625	94,149	53,036	51,734	4,111
	100	4.8	21,447	21,447	95,040	56,736	54,269	8,154
	1,000	47.9	36,728	36,728	111,348	124,298	99,288	81,746
	2,000	95.8	53,790	53,790	129,506	199,398	149,377	163,424
	6,000	287.3	121,763	121,763	202,071	499,592	349,667	490,342
	18,000	861.8	325,821	325,821	419,901	1,400,311	950,465	1,471,094
Center Bent	5	0.24	19,803	19,803	93,327	49,610	49,473	411
	50	2.4	20,625	20,625	94,149	53,036	51,734	4,111
	100	4.8	21,447	21,447	95,040	56,736	54,269	8,154
	1,000	47.9	36,728	36,728	111,348	124,298	99,288	81,746
	2,000	95.8	53,790	53,790	129,506	199,398	149,377	163,424
	6,000	287.3	121,763	121,763	202,071	499,592	349,667	490,342
	18,000	861.8	325,821	325,821	419,901	1,400,311	950,465	1,471,094
East Bent	5	0.24	19,803	19,803	93,327	49,610	49,473	411
	50	2.4	20,625	20,625	94,149	53,036	51,734	4,111
	100	4.8	21,447	21,447	95,040	56,736	54,269	8,154
	1,000	47.9	36,728	36,728	111,348	124,298	99,288	81,746
	2,000	95.8	53,790	53,790	129,506	199,398	149,377	163,424
	6,000	287.3	121,763	121,763	202,071	499,592	349,667	490,342
	18,000	861.8	325,821	325,821	419,901	1,400,311	950,465	1,471,094
East Abut	5	0.24	78,732	84,830	319,928	1,279,027	1,279,644	2,878
	50	2.4	81,609	87,708	323,012	1,294,239	1,300,132	28,985
	100	4.8	84,830	90,860	326,369	1,311,095	1,322,881	57,901
	1,000	47.9	142,457	148,555	387,628	1,614,578	1,732,367	579,077
	2,000	95.8	206,525	212,623	455,670	1,951,774	2,187,352	1,158,223
	6,000	287.3	462,727	468,826	727,907	3,300,693	4,007,427	3,474,601
	18,000	861.8	1,231,405	1,237,434	1,544,618	7,347,451	9,467,515	10,423,736

Earthquake Ground Motion Response Spectra

In an effort to characterize the response of the bridges with respect to the four earthquakes, an acceleration response spectrum (ARS) and displacement response spectrum (DRS) were created in the program SPECTRA (Carr, 2004) for each earthquake. The equivalent viscous damping was set at 5% of critical; the same value used in the bridge models. Figures 23 and 23 show the ARS and DRS for the transverse and longitudinal directions of the; Olympia, WA, Mexico City, Mexico, Kobe, Japan, Moquegua, Peru and Llolleo, Chile earthquake ground motions, respectively.

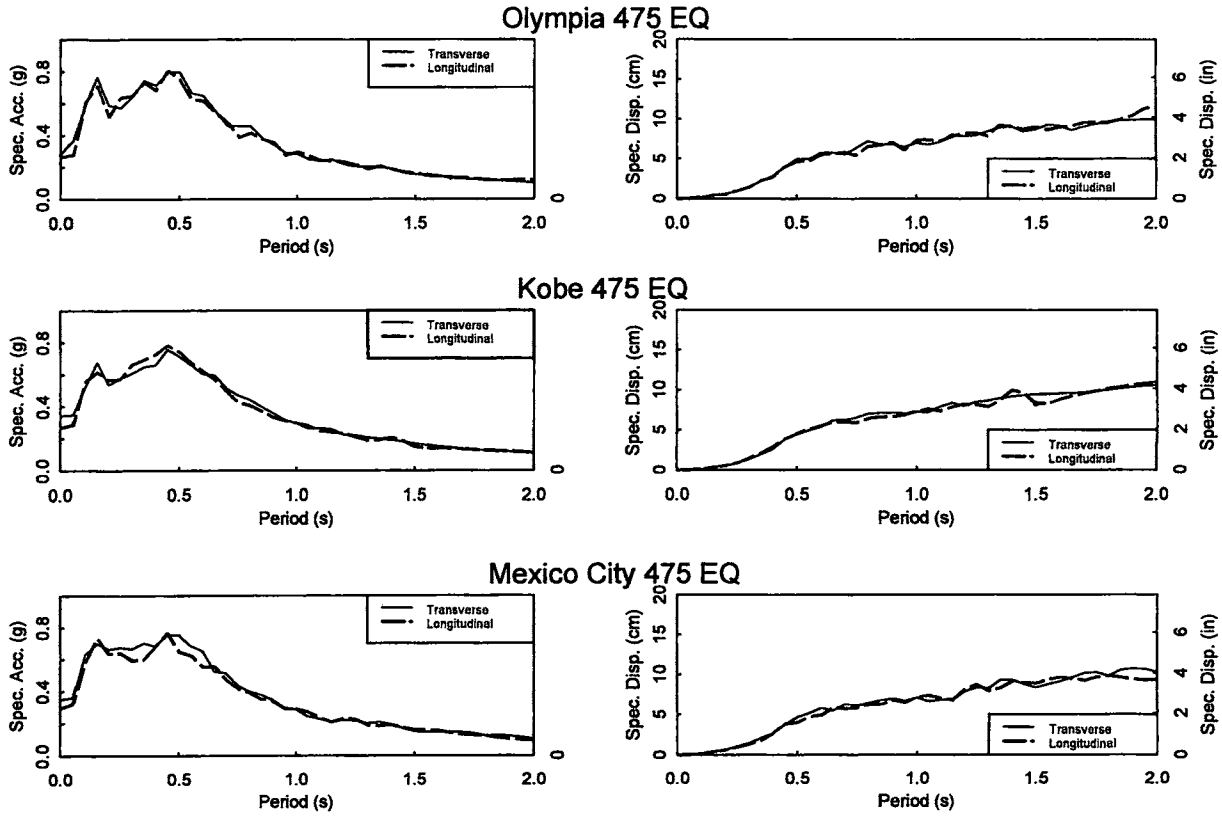

Figure 22 ARS and DRS of Olympia, WA, Kobe, Japan and Mexico City, Mexico Earthquake Ground Motions

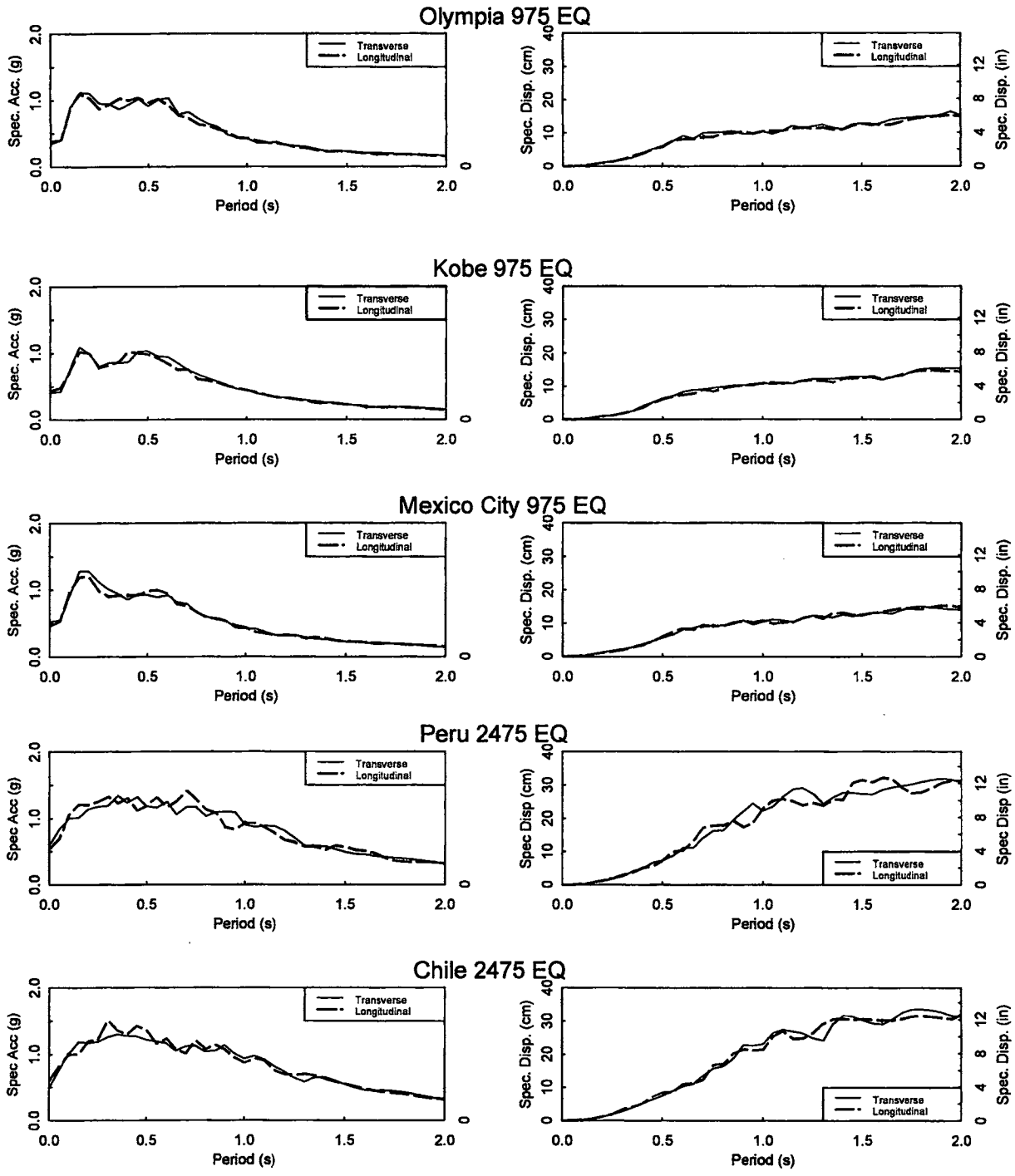

Figure 23 ARS and DRS of Olympia, WA, Kobe, Japan, Mexico City, Mexico, Moquegua, Peru, and Llolleo, Chile Earthquake Ground Motions

Table 4 shows the fundamental period for each controlling mode in the transverse, longitudinal and vertical directions of the bridges. All bridges with the respective soil stiffnesses are presented. For the soil-structure-interaction study, additional models for bridges 5/518, 5/227 and 5/826 with fixed conditions at the column foundation footings and roller/constrained conditions at the abutments (roller in the longitudinal direction of the bridge and constrained in the transverse and vertical axes) were included.

Table 4 Bridge Periods and Controlling Modes

		Transverse Dir.		Longitudinal Dir.		Vertical Dir.	
Bridge Model	**E_s-Ksi (MPa)**	**Period (s)**	**Mode**	**Period (s)**	**Mode**	**Period (s)**	**Mode**
5/518	1,000 (47.9)	0.705	1	0.561	3	0.293	6
	6,000 (287.3)	0.635	1	0.541	2	0.276	6
	18,000 (861.8)	0.625	1	0.537	2	0.274	6
	Fixed Column Roller/Abut	0.620	2	0.843	1	0.273	7
5/826	100 (4.8)	0.552	2	0.631	1	0.167	4
	1,000 (47.9)	0.512	2	0.600	1	0.161	4
	18,000 (861.8)	0.495	2	0.580	1	0.151	4
	Fixed Column Roller/Abut	0.492	2	0.870	1	0.149	4
5/227	5 (0.24)	0.419	1	0.342	3	0.125	14
	1,000 (47.9)	0.396	1	0.335	3	0.124	14
	18,000 (861.8)	0.373	1	0.328	3	0.123	14
	Fixed Column Roller/Abut	0.370	2	0.524	1	0.123	14

Bridge Seismic Assessment

The purpose of these nonlinear time history analyses was to assess the seismic vulnerability of the bridges. For all bridges, the subduction-zone earthquake ground motions (Peru or Chile) that imposed the largest demand on each bridge were used to evaluate the bridges. The Moquegua, Peru ground motions governed for all three bridges. Additionally, the 475-year and 975-year return period earthquake ground motions (Kobe, Olympia or Mexico

City) that imposed the largest demand on each bridge was used. For bridge 5/518 and 5/227, this was the Olympia, WA ground motions. The controlling earthquake ground motions for bridge 5/826 was Mexico City, Mexico.

Bridge 5/518 Model

Hysteresis curves are shown for the center bent, northern columns subjected to the Moquegua, Peru and Olympia, WA earthquake ground motions in Figures 24 and 25, respectively. Maximum column displacement, shear force, moment, and curvature demands are listed in Tables 5 and 6. For all the soil types studied, the displacement and shear force demand was higher in the transverse direction than in the longitudinal direction. As the soil spring stiffnesses were increased, the overall shape of the hysteresis curves did not change significantly. The column shear capacity was almost exceeded for the transverse direction of the center bent columns; shear failure of the columns is probable under the Moquegua, Peru earthquake ground motions. For the Olympia, WA earthquake ground motions, the column shear force demand did not approach the column shear capacity envelope.

For the Moquegua, Peru earthquake ground motions, the displacements varied as the soil spring stiffnesses increased. The maximum transverse displacement at the west bent decreased 6% from E_s = 1000 ksf (47.9 MPa) to E_s = 6000 ksf (287.3 MPa). This change was 19% when E_s was increased to 18000 ksf (862.8 MPa). Because the east bent columns are 2.5 ft (0.76 m) shorter than the west and center bent columns, the east bent had smaller maximum displacements in the transverse and longitudinal directions than those of the center or west bent. For all soil spring stiffnesses, the maximum transverse displacements were larger than the longitudinal displacements. Similar trends were seen in the Olympia, WA earthquake ground motions analysis results. All the bridge 5/518 bearing pads failed under the Moquegua, Peru earthquake

ground motions for all soil spring stiffness values. The abutment bearing pads experienced larger displacements than the bridge bent bearing pads for all soil spring stiffnesses. As the soil spring stiffnesses increased, the bearing pad displacement demand became more equalized between the abutments and bents. Failure in the bearing pads was defined by a bearing pad displacement greater than 1.44 in. (3.66 cm). The Olympia, WA earthquake resulted in similar bearing pad trends. The abutment bearing pads experienced higher demand than the bents. However, as the spring stiffnesses increased, the displacement demand did not shift as dramatically from the abutments to the bents as in the Moquegua, Peru earthquake. The largest difference in bearing pad displacement was 14% when comparing soil stiffness values of E_s = 100 ksf (47.9 MPa) to E_s = 18000 ksf (861.8 MPa). For all E_s values, failure occurred in the abutment bearing pads and sometimes in the outer bent bearing pads.

Column shear forces did not change significantly as the soil spring stiffnesses increased. For all E_s values, the maximum longitudinal and transverse shear force in the east and center bent was larger than the west bent. This was due to the higher displacement demand at the center bent and shorter column heights at the east bent. For the Moquegua, Peru earthquake, the largest difference in total column shear force as soil spring stiffnesses changed was 4%. For the Olympia, WA earthquake, the largest difference was 8%. For each soil spring stiffness, the center bent experienced the largest column moments.

For further study, an analysis of bridge 5/518 was performed with the column footings fixed and the abutments modeled with rollers in the longitudinal direction and constrained conditions in the transverse and vertical directions. For this study, the Moquegua, Peru earthquake ground motions were used. Figure 26 shows the center bent, center column hysteresis curves with the boundary conditions described above. When comparing the hysteresis

curves of the model with soil spring stiffnesses based on E_s = 6000 ksf (287.3 MPa) to the model with the fixed columns and roller/constrained abutments, the center bent saw a 22% and 6% increase in maximum transverse and longitudinal displacements, respectively, when the simplified boundary conditions were used. There was a 12% and 7% difference in the transverse and longitudinal shear force demand, respectively. Results from this study showed that the response of bridge 5/518 was sensitive to the variation in soil spring stiffness values. Using accurate soil spring stiffnesses was essential in obtaining correct demands on the bridge.

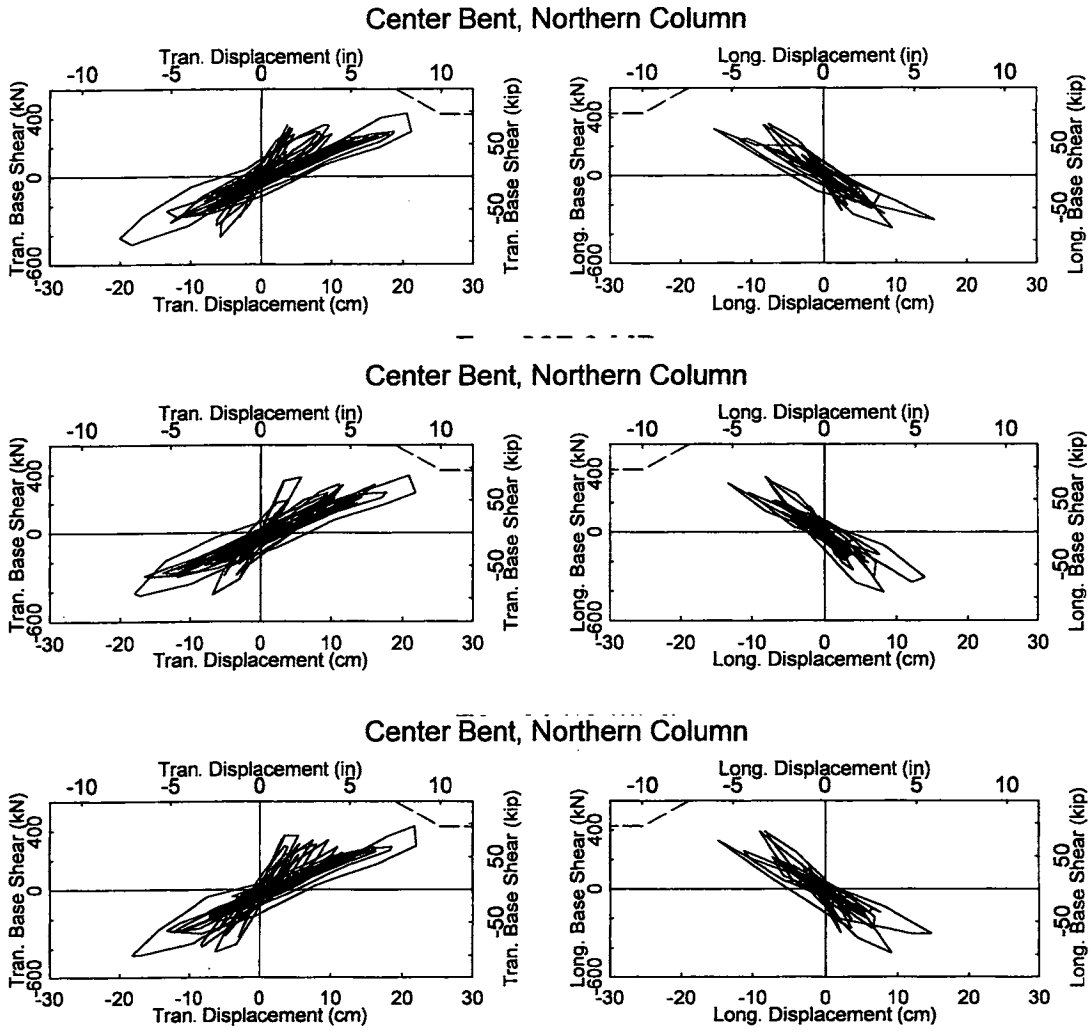

Figure 24 Center Bent, Northern Column: Hysteresis Curves for Bridge 5/518; Moquegua, Peru EQ; E_s = 1,000 Ksf; 6,000 Ksf; and 18,000 Ksf

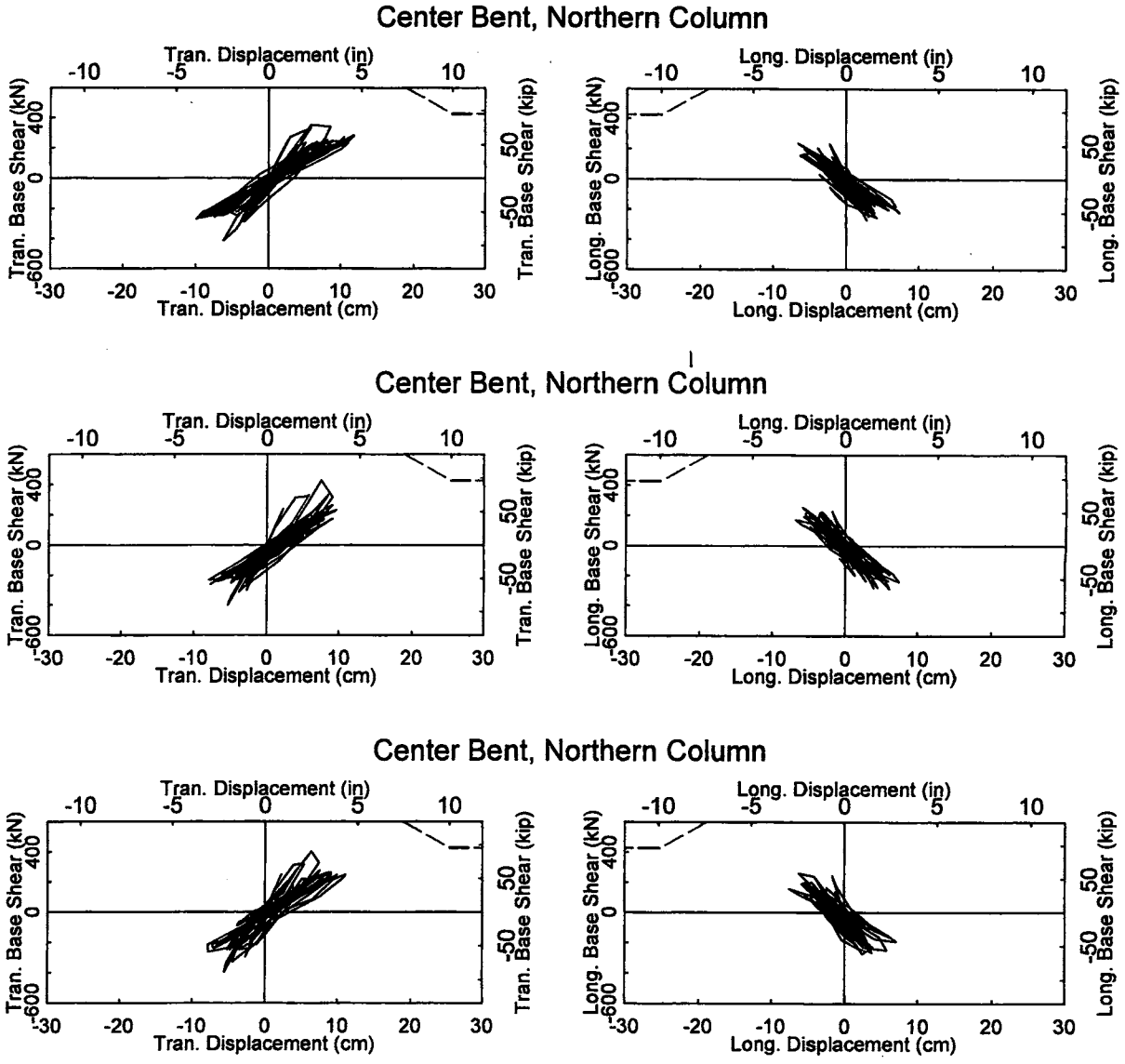

Figure 25 Center Bent, Northern Column: Hysteresis Curves for Bridge 5/518; Olympia, WA EQ; E_s = 1,000 Ksf; 6,000 Ksf; and 18,000 Ksf

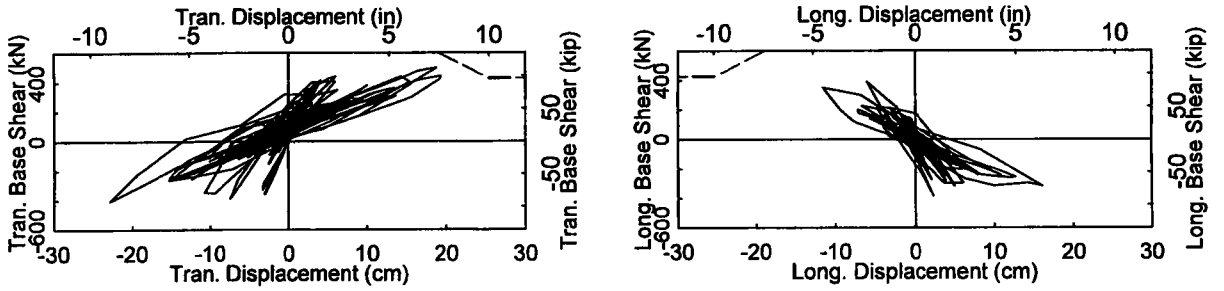

Figure 26 Center Bent, Center Column: Hysteresis Curves for Bridge 5/518; Moquegua, Peru EQ; Fixed Condition at Column Footings, Roller in Y and Constrained in X and Z Conditions at the Abutment

Table 5 Bridge 5/518 Column Displacement (Δ), Shear (V), Moment (M), and Curvature (ϕ) Demands; Moquegua, Peru EQ

Bent	**E_s = 47.9 MPa**			**E_s = 287.3 MPa**			**E_s = 861.8 MPa**		
Max Δ (cm)	**Tran Δ**	**Long Δ**	**Total Δ**	**Tran Δ**	**Long Δ**	**Total Δ**	**Tran Δ**	**Long Δ**	**Total Δ**
West	18.4-n	13.6-n	18.5-n	17.3-c	13.5-n	17.4-s	15.5-c	13.0-n	16.7-n
Center	21.2-n	15.6-n	23.4-s	20.4-s	15.4-s	22.9-n	21.9-n	15.6-s	24.3-s
East	12.3-s	11.2-s	12.6-n	14.0-n	10.8-n	14.1-s	11.2-s	10.4-n	12.2-n
Exp Joint/ Bearing Pad	**Gap Closing**	**Max Δ (cm)**	**Failure**	**Gap Closing**	**Max Δ (cm)**	**Failure**	**Gap Closing**	**Max Δ (cm)**	**Failure**
West Abut	Y	9.7	Y	Y	9.5	Y	Y	8.9	Y
West Bent	Y	5.7	Y	Y	5.6	Y	Y	5.6	Y
Center Bent	Y	3.5	Y	Y	3.8	Y	Y	4.1	Y
East Bent	Y	5.6	Y	Y	6.3	Y	Y	6.4	Y
East Abut	Y	7.6	Y	Y	7.2	Y	Y	6.9	Y
Max V (kN)	**Tran V**	**Long V**	**Total V**	**Tran V**	**Long V**	**Total V**	**Tran V**	**Long V**	**Total V**
West	422-n	366-n	444-n	426-s	378-c	426-s	411-n	352-n	438-n
Center	472-s	401-c	487-s	486-c	427-c	493-c	489-c	433-n	496-c
East	477-n	452-c	479-n	463-s	423-s	477-s	497-c	433-c	498-c
Total V (kN)	2799	2754	3718	2881	2532	3728	2801	2708	3725
Max Bot M (kN-m)	**Tran M**	**Long M**	**Total M**	**Tran M**	**Long M**	**Total M**	**Tran M**	**Long M**	**Total M**
West	1513-s	1710-c	1730-c	1398-c	1593-s	1676-n	1548-s	1706-c	1855-s
Center	1670-n	1950-n	1961-n	1763-c	2034-s	2034-s	1651-n	1936-c	1962-c
East	1510-c	1563-s	1653-s	1430-c	1763-c	1802-s	1486-n	1777-n	1811-n
Max Top M (kN-m)	**Tran M**	**Long M**	**Total M**	**Tran M**	**Long M**	**Total M**	**Tran M**	**Long M**	**Total M**
West	1566-c	1811-n	1815-n	1494-s	1719-c	1851-c	1734-n	1655-c	1990-c
Center	1875-n	1979-n	2042-n	1661-s	1852-c	1982-s	1741-n	1982-n	2030-n
East	1565-c	1741-c	1829-c	1462-n	1779-c	1779-c	1382-n	1764-s	1829-s
Max Top ϕ (1/m)	**Tran ϕ**	**Long ϕ**	**Total ϕ**	**Tran ϕ**	**Long ϕ**	**Total ϕ**	**Tran ϕ**	**Long ϕ**	**Total ϕ**
West	0.062	0.085	0.098	0.059	0.089	0.102	0.056	0.079	0.092
Center	0.082	0.121	0.135	0.075	0.115	0.121	0.085	0.121	0.131
East	0.072	0.085	0.102	0.072	0.095	0.115	0.075	0.095	0.115

Table 6 Bridge 5/518 Displacement (Δ), Shear (V), Moment (M), and Curvature (ϕ) Demands; Olympia, WA EQ

Bent	E_s = 47.9 MPa			E_s = 287.3 MPa			E_s = 861.8 MPa		
Max Δ (cm)	**Tran Δ**	**Long Δ**	**Total Δ**	**Tran Δ**	**Long Δ**	**Total Δ**	**Tran Δ**	**Long Δ**	**Total Δ**
West	8.2-n	6.3-s	8.6-s	9.2-c	6.2-n	9.4-s	7.1-c	5.9-n	7.1-s
Center	11.8-c	7.4-s	12.0-c	9.6-c	7.7-s	10.8-s	11.1-s	7.6-s	11.2-s
East	9.9-c	5.2-n	10.0-n	10.5-n	6.7-s	10.5-n	7.6-s	5.3-n	7.6-s
Exp Joint/ Bearing Pad	**Gap Closing**	**Max Δ (cm)**	**Failure**	**Gap Closing**	**Max Δ (cm)**	**Failure**	**Gap Closing**	**Max Δ (cm)**	**Failure**
West Abut	Y	4.9	Y	Y	4.6	Y	Y	4.3	Y
West Bent	Y	3.9	Y	Y	4.4	N	Y	3.4	N
Center Bent	Y	2.3	N	Y	2.7	N	Y	2.7	N
East Bent	Y	3.5	N	Y	4.5	Y	Y	3.6	N
East Abut	Y	4.4	Y	Y	4.6	Y	Y	3.9	Y
Max V (kN)	**Tran V**	**Long V**	**Total V**	**Tran V**	**Long V**	**Total V**	**Tran V**	**Long V**	**Total V**
West	307-c	256-s	342-c	392-c	245-c	395-c	365-c	268s,n	367-c
Center	418-c	271-c	422-c	427s,n	290-c	427s,n	429-c	322-c	431-c
East	430-c	286-s	431-c	421s,n	373-n	423-n	423-n	351-n	422-n
Total V (kN)	2245	2039	3090	2934	2331	3636	3005	1903	3741
Max Bot M (kN-m)	**Tran M**	**Long M**	**Total M**	**Tran M**	**Long M**	**Total M**	**Tran M**	**Long M**	**Total M**
West	1340-n	1531-n	1650-s	1434-c	1502-c	1509-c	1460-c	1552-s	1617-c
Center	1566-s	1723-n	1856-c	1594-c	1703-n	1760-c	1574-c	1666-s	1887-n
East	1382-c	1436-n	1547-n	1401-n	1525-c	1607-c	1411-s	1491-s	1672-s
Max Top M (kN-m)	**Tran M**	**Long M**	**Total M**	**Tran M**	**Long M**	**Total M**	**Tran M**	**Long M**	**Total M**
West	1540-c	1475-s	1695-c	1489-c	1580-n	1585-s	1471-c	1512-s	1554-n
Center	1665-c	1763-s	1920-n	1617-c	1749-c	1787-c	1532-n	1679-s	1746-n
East	1402-s	1481-s	1491-s	1394-c	1449-c	1529-n	1456-c	1504-n	1504-n
Max Top ϕ (1/m)	**Tran ϕ**	**Long ϕ**	**Total ϕ**	**Tran ϕ**	**Long ϕ**	**Total ϕ**	**Tran ϕ**	**Long ϕ**	**Total ϕ**
West	0.043	0.046	0.059	0.046	0.056	0.062	0.059	0.059	0.069
Center	0.062	0.089	0.102	0.059	0.075	0.089	0.056	0.072	0.082
East	0.043	0.052	0.062	0.049	0.059	0.072	0.043	0.059	0.062

Bridge 5/826 Model

Bridge 5/826 has the largest column aspect ratios and largest transverse confinement ratio of the three bridges. In addition, Bridge 5/826 has a monolithic deck while the other two bridges have non-monolithic decks. Therefore, the displacement capacity of Bridge 5/826 exceeds that of the other two bridges. Hysteresis curves for the center bent, center columns subject to the

Moquegua, Peru and Mexico City, Mexico ground motions are shown in Figures 27 and 28, respectively. Maximum column displacement, shear force, moment, and curvature demands are listed in Tables 7 and 8. Looking first at the Moquegua, Peru results, when comparing the maximum total displacements for soil spring stiffnesses based on E_s = 100 ksf (4.8 MPa) and E_s = 18000 ksf (861.8 MPa), there was a total displacements reduction of 10% at the center bent as the soil spring stiffnesses increased. The trends in bridge maximum displacements were similar for the Mexico City, Mexico ground motions. For all E_s values, the maximum transverse displacement at the center bent was larger than the east and west bents. The maximum longitudinal displacements were larger than the maximum transverse displacements for all soil stiffness values. Bridge 5/826 was the only bridge that experienced larger demand in the longitudinal axis of the bridge than the transverse axis of the bridge. Because the bridge deck was monolithically constructed, the stiffness in the transverse axis of the bridge was larger than the bridges with non-monolithic bridge decks. As a result the first mode response occurred along the longitudinal axis of the bridge compared with the transverse first mode response of the other bridges (see Table 4).

For the Mexico City, Mexico and Moquegua, Peru ground motions, failure was predicted for both abutment bearing pads. The maximum bearing pad displacements were similar for all soil spring stiffness values. For both earthquakes, column shear forces and moments did not show trends as the soil spring stiffnesses increased. The shear force/displacement demands for the columns in bridge 5/826 did not approach the shear capacity envelope in any of the ground motions used in this study. This was largely due to the column aspect ratio of 4.2, the monolithic bridge deck and the transverse steel ratio of 0.43% compared with non-monolithic bridge decks for the other two bridges and lower column aspect ratios and transverse reinforcement ratios.

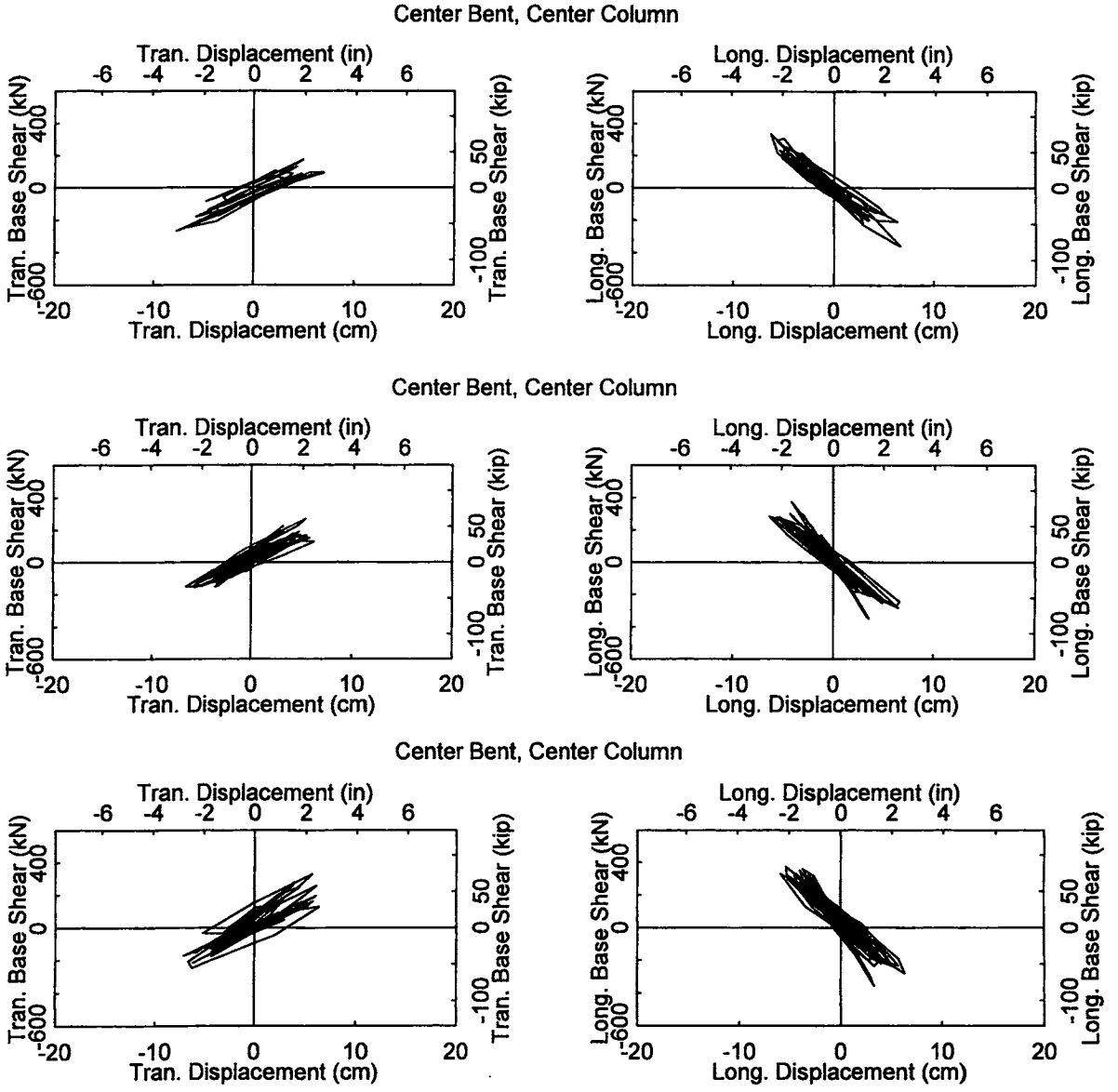

Figure 27 Center Bent, Center Column: Hysteresis Curves for Bridge 5/826; Mexico City, Mexico EQ; E_s = 100 Ksf; 1,000 Ksf; and 18,000 Ksf

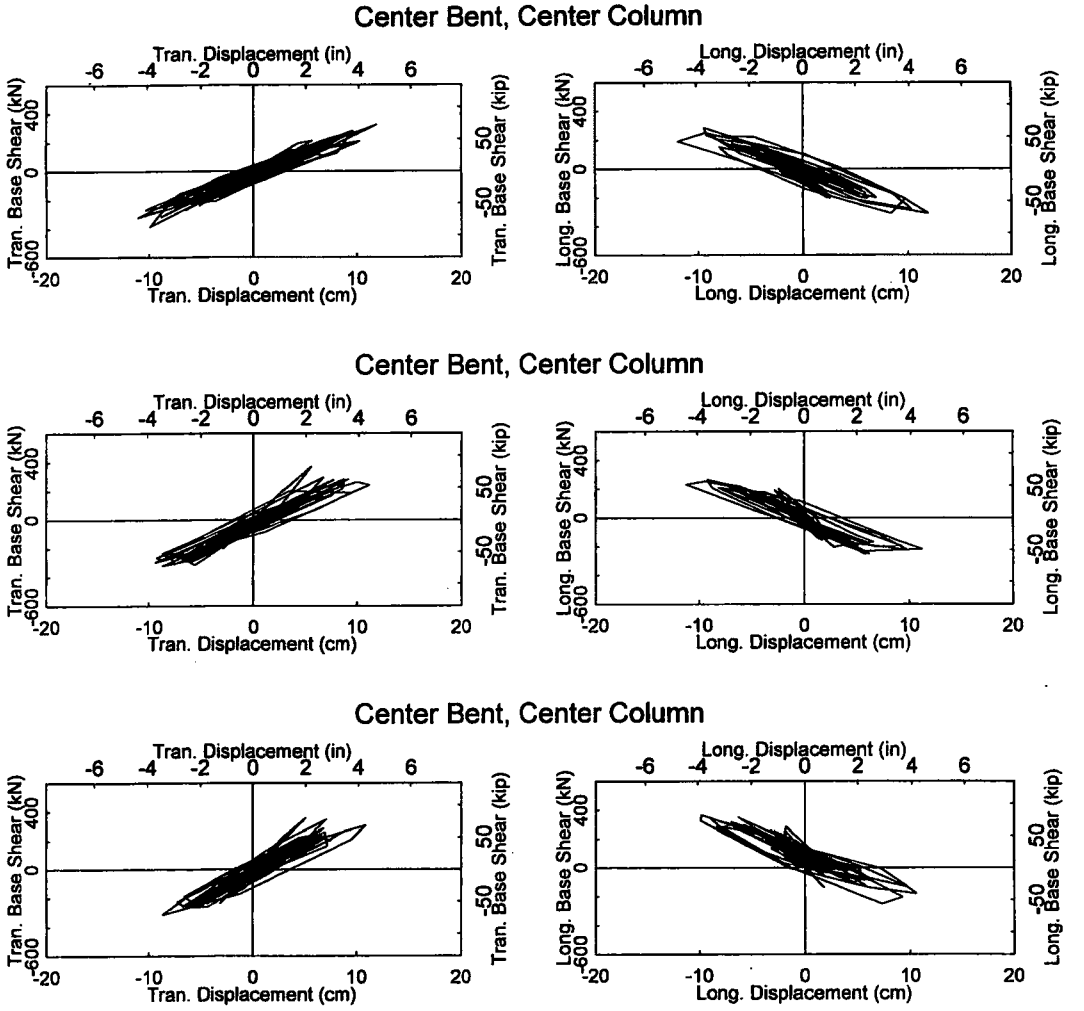

Figure 28 Center Bent, Center Column: Hysteresis Curves for Bridge 5/826; Moquegua, Peru EQ; E_s = 100 Ksf; 1,000 Ksf; and 18,000 Ksf

A model of bridge 5/826 with column footings fixed and the abutments modeled with rollers in the longitudinal direction and constrained conditions in the transverse and vertical directions was created and subjected to the Moquegua, Peru earthquake. Figure 29 shows the center bent, center column hysteresis curves for the boundary conditions described above. When comparing the hysteresis curves of the model with soil spring stiffnesses based on E_s = 1000 ksf (47.9 MPa) to the model with the fixed columns and roller/constrained abutments, the center bent

experienced 12% and 18% increases in the maximum transverse and longitudinal displacements, respectively, for the simplified boundary conditions.

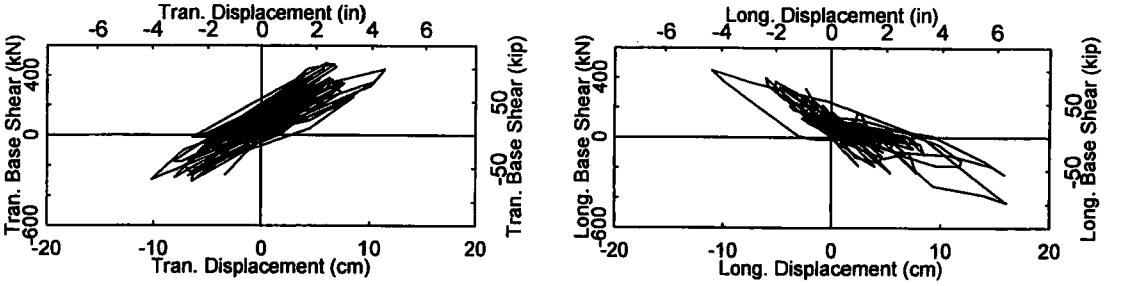

Figure 29 Center Bent, Southern Column: Hysteresis Curves for Bridge 5/826; Moquegua, Peru EQ; Fixed Condition at Column Footings, Roller in Y and Constrained in X and Z Conditions at the Abutment

Table 7 Bridge 5/826 Displacement (Δ), Shear (V), Moment (M), and Curvature (ϕ) Demands; Moquegua, Peru EQ

Bent	**E_s = 4.8 MPa**			**E_s = 47.9 MPa**			**E_s = 861.8 MPa**		
Max Δ (cm)	**Tran Δ**	**Long Δ**	**Total Δ**	**Tran Δ**	**Long Δ**	**Total Δ**	**Tran Δ**	**Long Δ**	**Total Δ**
West	7.2-n	12.4-s	12.8-s	6.5-n	11.6-s	11.9-s	6.0-n	11.0-s	11.2-s
Center	12.0-n	12.0-s	13.5-s	11.2-n	11.3-s	12.7-s	10.9-n	10.6-s	11.8-s
East	7.4-s	12.2-n	12.5-n	7.4-s	11.8-n	12.1-n	7.0-s	10.9-n	11.1-n
Exp Joint/ Bearing Pad	**Gap Closing**	**Max Δ (cm)**	**Failure**	**Gap Closing**	**Max Δ (cm)**	**Failure**	**Gap Closing**	**Max Δ (cm)**	**Failure**
West Abut	Y	12.0	Y	Y	11.1	Y	Y	10.6	Y
East Abut	Y	11.3	Y	Y	10.5	Y	Y	10.3	Y
Max V (kN)	**Tran V**	**Long V**	**Total V**	**Tran V**	**Long V**	**Total V**	**Tran V**	**Long V**	**Total V**
West	305-n	391-s	402-s	399-n	403-s	429-s	328-n	361-c	485-c
Center	397-c	355-n	404-c	372-c	363-s	443-c	357-c	413-n	494-n
East	323-s	340-c	363-s	303-s	382-s	415-s	302-c	412-n	454-n
Total V (kN)	2555	2429	3130	2737	2439	4131	2669	2651	3817
Max Bot M (kN-m)	**Tran M**	**Long M**	**Total M**	**Tran M**	**Long M**	**Total M**	**Tran M**	**Long M**	**Total M**
West	1603-s	1533-n	1805-c	2323-s	1889-n	2506-n	2542-s	3137-n	3144-n
Center	1929-s	1620-s	1933-s	3040-n	2525-c	3243-c	2285-s	2409-n	2873-n
East	1661-c	1439-s	1805-c	2375-c	2200-c	2698-c	2443-s	3236-c	3242-s
Max Top M (kN-m)	**Tran M**	**Long M**	**Total M**	**Tran M**	**Long M**	**Total M**	**Tran M**	**Long M**	**Total M**
West	12304s	1925-n	2739-s	2527-s	2144-c	2863-s	2789-n	3400-n	3415-n
Center	2154-s	2272-c	2680-s	2280-s	2769-c	3023-c	2214-c	2382-n	2778-n
East	2168-c	2114-s	2638-s	2454-c	2454-n	3047-c	2120-c	1955-c	2381-c
Max Top ϕ (1/m)	**Tran ϕ**	**Long ϕ**	**Total ϕ**	**Tran ϕ**	**Long ϕ**	**Total ϕ**	**Tran ϕ**	**Long ϕ**	**Total ϕ**
West	0.036	0.036	0.039	0.043	0.020	0.046	0.039	0.033	0.052
Center	0.033	0.039	0.046	0.033	0.056	0.056	0.033	0.036	0.043
East	0.033	0.039	0.043	0.043	0.030	0.049	0.043	0.030	0.049

Table 8 Bridge 5/826 Displacement (Δ), Shear (V), Moment (M), and Curvature (ϕ) Demands; Mexico City, Mexico EQ

Bent	E_s = 4.8 MPa			E_s = 47.9 MPa			E_s = 861.8 MPa		
Max Δ (cm)	**Tran Δ**	**Long Δ**	**Total Δ**	**Tran Δ**	**Long Δ**	**Total Δ**	**Tran Δ**	**Long Δ**	**Total Δ**
West	4.4-n	6.8-s	7.4-n	3.8-n	7.1-n	7.5-n	4.0-n	6.8-n	7.2-n
Center	7.8-n	6.7-s	9.4-n	6.7-n	6.7-s	7.9-n	7.2-n	6.4-n	8.1-n
East	4.5-s	6.6-n	7.3-s	4.4-s	6.9-s	7.4-s	4.6-s	6.7-s	7.4-s
Exp Joint/ Bearing Pad	**Gap Closing**	**Max Δ (cm)**	**Failure**	**Gap Closing**	**Max Δ (cm)**	**Failure**	**Gap Closing**	**Max Δ (cm)**	**Failure**
West Abut	Y	7.1	Y	Y	6.6	Y	Y	6.3	Y
East Abut	Y	6.6	Y	Y	6.2	Y	Y	6.1	Y
Max V (kN)	**Tran V**	**Long V**	**Total V**	**Tran V**	**Long V**	**Total V**	**Tran V**	**Long V**	**Total V**
West	268-n	368-c	368-c	304-c	374-c	374-n	386-s	412-s	421-s
Center	278-s	463-c	465-c	307-n	427-c	428-s	337-s	286-c	345-c
East	262-s	334-n	334-n	274-c	343-s	360-s	230-n	346-n	346-n
Total V (kN)	1315	2278	3131	2084	2980	3368	2217	2949	3720
Max Bot M (kN-m)	**Tran M**	**Long M**	**Total M**	**Tran M**	**Long M**	**Total M**	**Tran M**	**Long M**	**Total M**
West	1562-s	1089-c	1601-s	2045-s	1472-n	2209-c	1784-n	1615-c	1905-n
Center	1574-s	1369-n	1712-n	1924-s	2407-n	2455-c	1992-n	2027-c	2275-n
East	1062-c	941-s	1098-c	1978-n	1636-s	2062-n	2019-c	1593-s	2061-c
Max Top M (kN-m)	**Tran M**	**Long M**	**Total M**	**Tran M**	**Long M**	**Total M**	**Tran M**	**Long M**	**Total M**
West	1782-s	1719-c	1989-s	2022-c	1574-n	2213-c	1798-n	1590-c	1853-n
Center	3068-s	1948-n	3071-n	2609-c	2076-c	2670-c	2005-c	2070-s	2320-s
East	1824-s	1695-s	1829-s	1904-n	1623-c	2003-c	2019-s	1650-n	2061-c
Max Top ϕ (1/m)	**Tran ϕ**	**Long ϕ**	**Total ϕ**	**Tran ϕ**	**Long ϕ**	**Total ϕ**	**Tran ϕ**	**Long ϕ**	**Total ϕ**
West	0.030	0.026	0.033	0.036	0.023	0.039	0.033	0.013	0.036
Center	0.020	0.026	0.030	0.036	0.033	0.043	0.026	0.020	0.030
East	0.016	0.020	0.023	0.033	0.023	0.036	0.033	0.020	0.036

As soil spring stiffnesses increased, the maximum displacements did not show trends in values for all bents. When the bridge was modeled with fixed column bases and with rollers (along the longitudinal bridge axis) and constrained axes (along the vertical and transverse bridge axes) at the abutment, larger transverse and longitudinal displacements were noted at the east and west bents. Thus, modeling soil-structure-interaction with secant stiffness springs did

have an effect on the global response of bridge 5/826, but the specific soil spring stiffnesses used were not as influential.

Bridge 5/227 Model

Hysteresis curves for the center bent, center column for the Moquegua, Peru and Olympia, WA earthquake ground motions are shown in Figure 30 and Figure 31, respectively. Maximum column displacement, shear force, moment, and curvature demands are listed in Tables 9 and 10. Looking first at the Moquegua, Peru ground motion results, the transverse and longitudinal column displacements were reduced as the soil spring stiffnesses increased. The east bent experienced the largest decrease in maximum transverse displacement (31%). Similar results were seen in the Olympia, WA earthquake analysis. The west and east abutments saw the largest bearing pad displacement demands. For the Moquegua, Peru ground motions, the abutment bearing pads only failed in the model with soil spring stiffnesses based on E_s = 5 ksf (0.24 MPa). No bearing pads failed for the Mexico City, Mexico earthquake ground motions.

For the Moquegua, Peru earthquake ground motions, maximum transverse column shear forces remained similar. The Olympia, WA earthquake ground motions resulted in similar trends in maximum column shear forces. Under the Moquegua, Peru and Olympia, WA earthquake ground motions, the maximum moments were similar for each soil value as well. Based on the column force/displacement curves in Figure 28, it is likely that column shear failure would occur in bridge 5/227 under the Moquegua, Peru earthquake ground motions. The column shear forces did not approach the shear capacity envelope for the Olympia, WA earthquake ground motions.

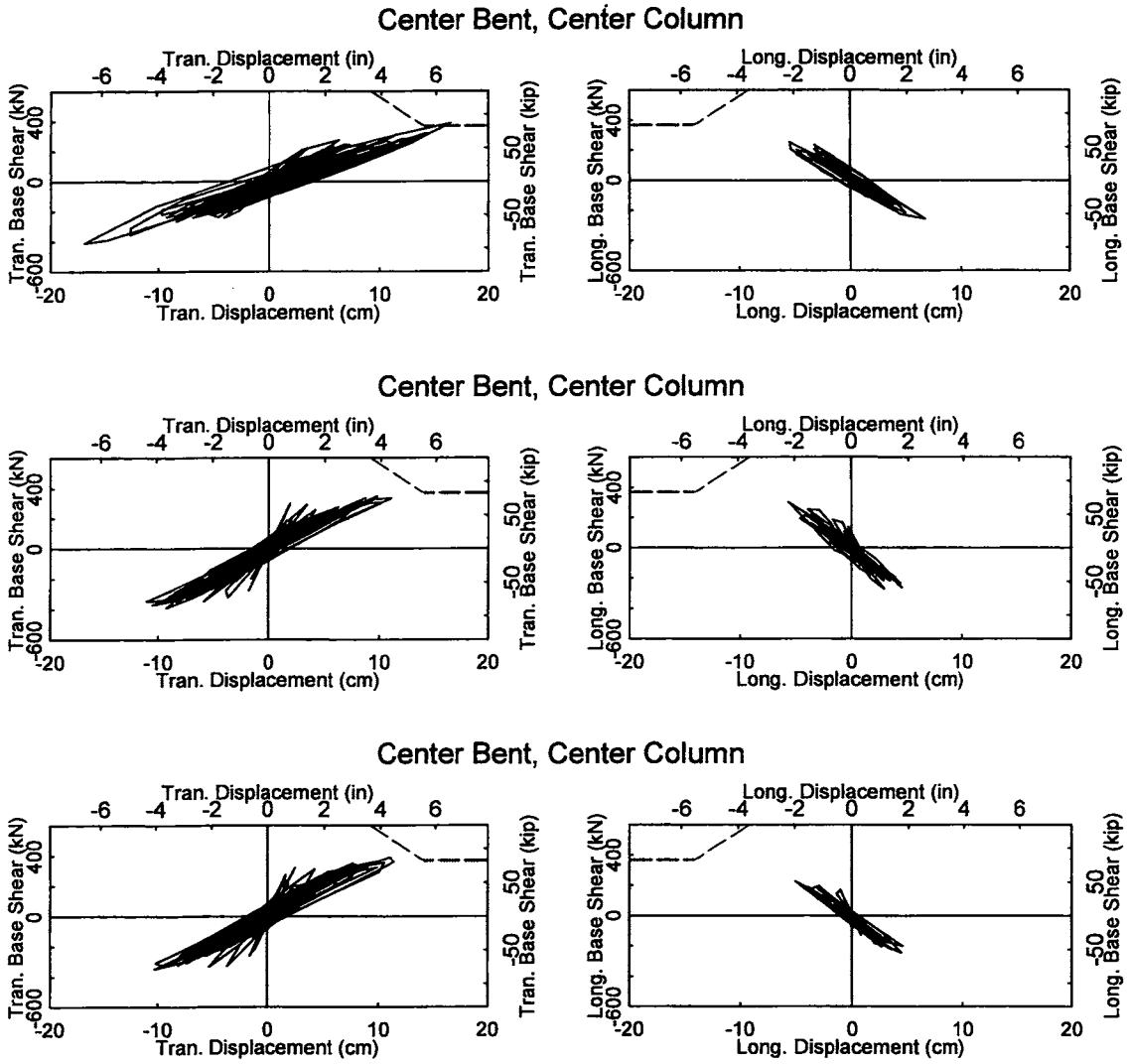

Figure 30 Center Bent, Center Column: Hysteresis Curves for Bridge 5/227; Moquegua, Peru EQ; E_s = 5 Ksf; 1,000 Ksf; and 18,000 Ksf

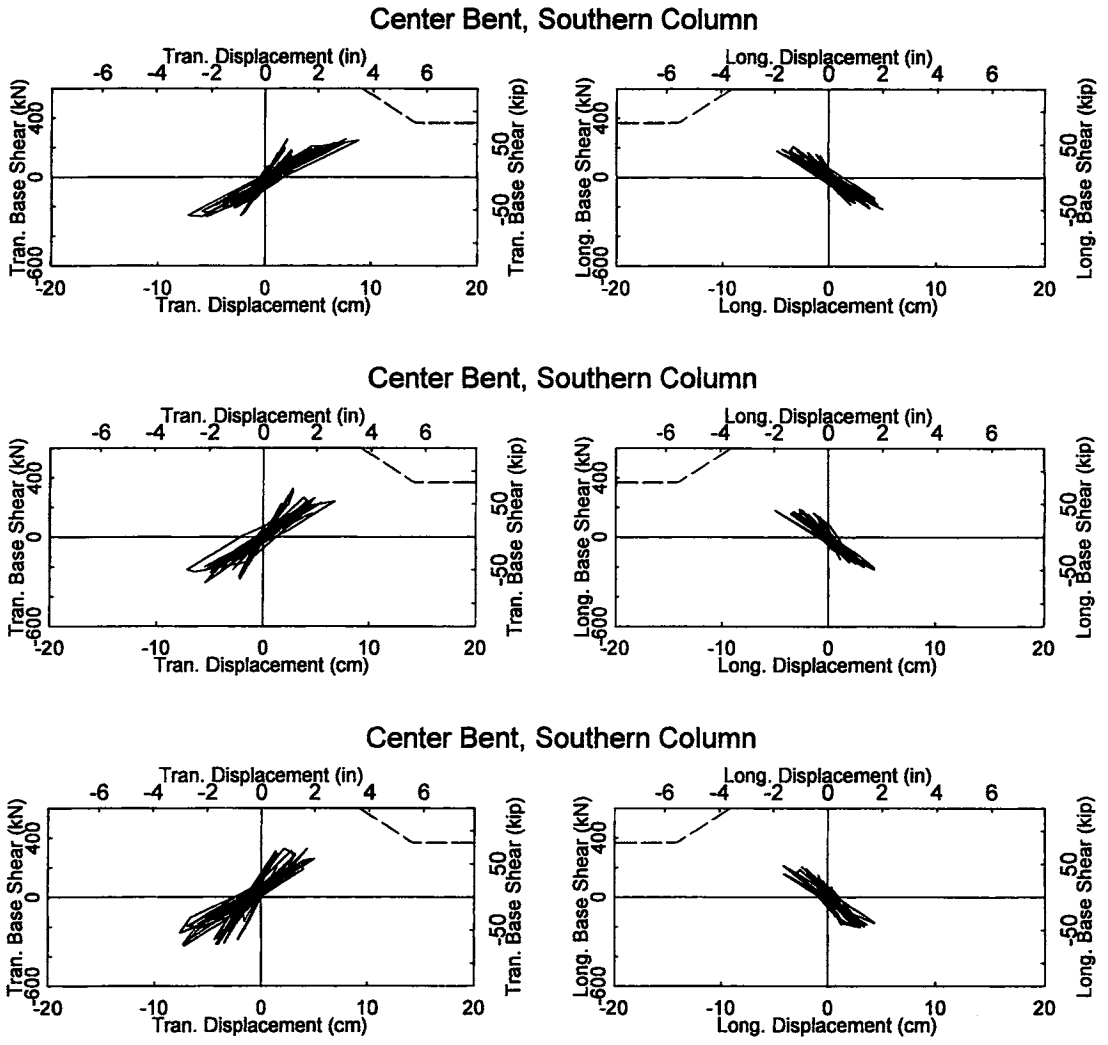

Figure 31 Center Bent, Southern Column: Hysteresis Curves for Bridge 5/227; Olympia, WA EQ; E_s = 5 Ksf; 1,000 Ksf; and 18,000 Ksf

A model of bridge 5/227 with column footings fixed and the abutments modeled with rollers in the longitudinal direction and constrained conditions in the transverse and vertical directions was also created. For this study, the Moquegua, Peru earthquake ground motions were used. Figure 32 shows the center bent, center northern column hysteresis curves for the boundary conditions described above. When comparing the hysteresis curves of the model with soil spring stiffnesses based on E_s = 1000 ksf (47.9 MPa) to the model with the fixed columns

and roller/constrained abutments, the center bent experienced a 27% decrease and a 60% increase in maximum negative transverse and longitudinal displacements, respectively. The hysteretic response of the center bent columns showed that the transverse and longitudinal shear capacity envelopes were nearly reached for the model with roller/constrained abutment boundary conditions. Conversely, only the transverse direction force/displacement response was governing in the models with soil-structure interaction included.

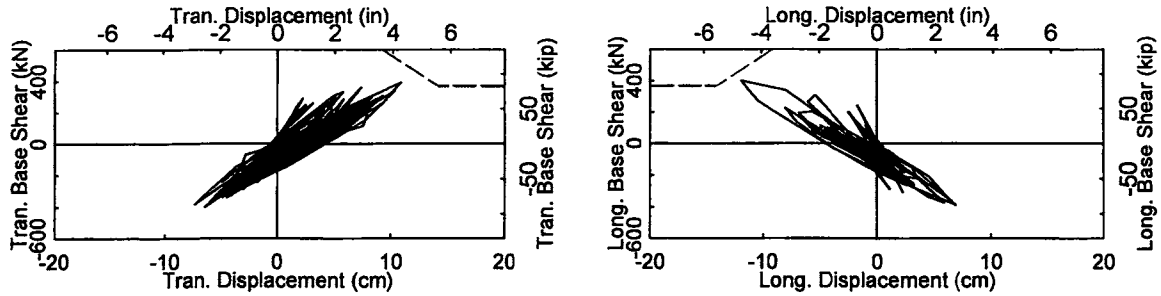

Figure 32 Center Bent, Northern Column: Hysteresis Curves for Bridge 5/227; Moquegua, Peru EQ; Fixed Condition at Column Footings, Roller in Y and Constrained in X and Z Conditions at the Abutment

The results for bridge 5/227 showed that the response of the bridge was sensitive to soil-structure-interaction. There was a trend in reduction of transverse displacement demand as soil spring stiffnesses increased. The foundations for bridge 5/227 were much different than those of bridges 5/518 and 5/826. For bridge 5/518, only the east abutment has two sub-ground spread footings. For bridge 5/227, both abutments have two sub-ground pile footings. Bridge 5/826 has piles underneath the abutment spread footing. The soil spring stiffnesses were significantly larger for bridge 5/227 because of the concrete piles. Also, bridge 5/227 is much shorter in length and has shorter columns than bridges 5/518 and 5/826. Thus, comparing the sensitivity of soil-structure-interaction of bridge 5/227 to bridges 5/518 or 5/826 cannot directly be done. However, it can be stated that soil-structure-interaction had a significant effect on each bridge

and must be accounted for to accurately assess the bridge response to seismic excitations. The thesis "Seismic Assessment and Retrofit of Existing Multi-Column Bent Bridges" (Cox, 2005) can be referenced for more detailed information on the modeling and analysis of the three bridges.

Table 9 Bridge 5/227 Displacement (Δ), Shear (V), Moment (M), and Curvature (ϕ) Demands; Moquegua, Peru EQ

Bent	E_s = 0.24 MPa			E_s = 47.9 MPa			E_s = 861.8 MPa		
Max Δ (cm)	**Tran Δ**	**Long Δ**	**Total Δ**	**Tran Δ**	**Long Δ**	**Total Δ**	**Tran Δ**	**Long Δ**	**Total Δ**
West	9.7-c	5.1-s,n	9.9-c	9.7-s,n	4.1-s,n	9.9-s,n	8.6-c	4.6-n	8.6-s
Center	13.7-s	7.1-s	14.0-n	11.2-s,n	5.6-s,n	11.2-s,n	11.4-c	5.0-c	11.5-c
East	7.9-s	4.8-s	7.9-s,n	7.1-n	4.3-s,n	7.1-n	7.1-c	3.1-c	5.5-s,n
Exp Joint/ Bearing Pad	**Gap Closing**	**Max Δ (cm)**	**Failure**	**Gap Closing**	**Max Δ (cm)**	**Failure**	**Gap Closing**	**Max Δ (cm)**	**Failure**
West Abut	Y	3.9	Y	Y	3.5	N	Y	3.1	N
West Bent	Y	3.3	N	Y	3.2	N	Y	2.7	N
Center Bent	Y	1.6	N	Y	1.5	N	Y	1.7	N
East Bent	Y	2.7	N	Y	2.5	N	Y	3.2	N
East Abut	Y	3.9	Y	Y	3.5	N	Y	2.6	N
Max V (kN)	**Tran V**	**Long V**	**Total V**	**Tran V**	**Long V**	**Total V**	**Tran V**	**Long V**	**Total V**
West	312-c	285-s,n	332-c	316-c	315-c	347-c	335-c	312-s,n	360-c
Center	381-c	322-c	403-c	389-c	301-c	399-c	387-c	300-s,n	417-c
East	394-c	292-c	399-c	396-c	386-c	401-c	372-c	351-s,n	377-c
Total V (kN)	2721	2163	3422	2717	2257	2805	2427	2260	2776
Max Bot M (kN-m)	**Tran M**	**Long M**	**Total M**	**Tran M**	**Long M**	**Total M**	**Tran M**	**Long M**	**Total M**
West	1207-c	1649-c	1832-c	1219-c	1723-c	1891-c	1166-n	1657-c	1645-n
Center	1276-c	1893-n	2011-s	1254-c	1927-c	2028-c	1279-c	1982-c	2030-c
East	1104-n	1415-c	1542-c	1075-c	1262-s	1422-c	1070-n	1220-c	1402-c
Max Top M (kN-m)	**Tran M**	**Long M**	**Total M**	**Tran M**	**Long M**	**Total M**	**Tran M**	**Long M**	**Total M**
West	1357-c	1787-c	1897-c	1260-c	1742-c	1791-c	1169-c	1711-c	1798-c
Center	1331-c	2011-c	2138-c	1291-c	2065-c	2225-c	1255-c	2047-c	2118-c
East	1197-n	1517-n	1636-n	1129s,n	1456s,n	1552-n	1049-c	1291-c	1481-c
Max Top ϕ (1/m)	**Tran ϕ**	**Long ϕ**	**Total ϕ**	**Tran ϕ**	**Long ϕ**	**Total ϕ**	**Tran ϕ**	**Long ϕ**	**Total ϕ**
West	0.043	0.092	0.095	0.039	0.085	0.089	0.036	0.082	0.085
Center	0.062	0.115	0.121	0.039	0.121	0.125	0.043	0.108	0.112
East	0.039	0.079	0.085	0.036	0.072	0.075	0.020	0.046	0.049

Table 10 Bridge 5/227 Displacement (Δ), Shear (V), Moment (M), and Curvature (ϕ) Demands; Olympia, WA EQ

Bent	E_s = 0.24 MPa			E_s = 47.9 MPa			E_s = 861.8 MPa		
Max Δ (cm)	**Tran Δ**	**Long Δ**	**Total Δ**	**Tran Δ**	**Long Δ**	**Total Δ**	**Tran Δ**	**Long Δ**	**Total Δ**
West	4.8-s,n	3.8-s,n	5.1-c	5.3-s,n	3.6-c	5.6-s,n	4.1-s,n	3.3-s,n	4.5-c
Center	8.9-s	5.1-s	9.0-s	7.1-c	5.0-c	7.1-c	7.6-s	4.4-s	7.8-n
East	5.3-c	3.4-c	6.0-c	5.1-c	3.2-n	6.0-n	4.6-s,n	2.9-s,n	5.3-s,n
Exp Joint/ Bearing Pad	**Gap Closing**	**Max Δ (cm)**	**Failure**	**Gap Closing**	**Max Δ (cm)**	**Failure**	**Gap Closing**	**Max Δ (cm)**	**Failure**
West Abut	Y	3.1	N	Y	3.0	N	Y	2.7	N
West Bent	Y	2.0	N	Y	2.2	N	Y	2.2	N
Center Bent	Y	1.6	N	Y	1.5	N	Y	1.5	N
East Bent	Y	2.4	N	Y	2.6	N	Y	3.0	N
East Abut	Y	2.7	N	Y	2.9	N	Y	2.9	N
Max V (kN)	**Tran V**	**Long V**	**Total V**	**Tran V**	**Long V**	**Total V**	**Tran V**	**Long V**	**Total V**
West	293-c	223-c	318-c	311-s,n	282-c	316-c	307-s,n	308-c	312-c
Center	335-c	231-c	335-c	361-c	260-c	377-c	338-n	277-n	351-n
East	314-c	236-c	321-c	324-c	226-n	325-c	298-s,n	270-c	360-c
Total V (kN)	2057	1718	3243	2507	1830	3179	1990	1764	2971
Max Bot M (kN-m)	**Tran M**	**Long M**	**Total M**	**Tran M**	**Long M**	**Total M**	**Tran M**	**Long M**	**Total M**
West	1205s,n	1171s,n	1433s,n	1142-c	1272-c	1510-c	1161-c	1171s,n	1406-c
Center	1288-c	1597-c	1702-s	1331-c	1281s,n	1428s,n	1212-n	1609-c	1627-c
East	1070s,n	1298s,n	1319s,n	1136-c	1321-n	1531-c	1148-c	1269-c	1265-c
Max Top M (kN-m)	**Tran M**	**Long M**	**Total M**	**Tran M**	**Long M**	**Total M**	**Tran M**	**Long M**	**Total M**
West	1152-c	1390-c	1505-c	1230-c	1356-c	1525s,n	1215-c	1227-c	1363-c
Center	1292-c	1558-n	1654-c	1315-c	1237s,n	1467s,n	1270-s	2214-c	1536-s
East	1193-c	1257-c	1449-c	1174-n	1310-s	1453-c	1081-c	1253-c	1367-c
Max Top ϕ (1/m)	**Tran ϕ**	**Long ϕ**	**Total ϕ**	**Tran ϕ**	**Long ϕ**	**Total ϕ**	**Tran ϕ**	**Long ϕ**	**Total ϕ**
West	0.036	0.049	0.056	0.036	0.046	0.056	0.033	0.036	0.049
Center	0.056	0.079	0.082	0.046	0.052	0.062	0.043	0.069	0.079
East	0.036	0.052	0.062	0.033	0.049	0.066	0.030	0.046	0.046

WSU-NEABS/RUAUMOKO Comparison

In recent research performed by Thompson (2004), bridges 5/518 and 5/826 were also analyzed using the program WSU-NEABS (Zhang et.al., 1999)and the Moquegua, Peru, ground motions. Thompson's soil spring stiffnesses for bridge 5/518 were similar to the model in this research based on E_s = 287.3 MPa (6000 ksf). Thompson's soil spring stiffnesses for bridge 5/826 were similar to the values used in this research based on E_s = 47.9 MPa (100 ksf). Results from WSU- NEABS using the Moquegua, Peru ground motions showed some differences with the results in this study using RUAUMOKO, however, the overall bridge assessments were similar. When comparing the analyses of bridge 5/518, the maximum total column displacement at the center bent varied by less than 20%. The maximum total column shear force at the center bent varied by less than 10%. When comparing analyses of bridge 5/826, for WSU-NEABS, the maximum total column displacement at the center bent varied by less than 15%. The maximum total column shear force at the center bent varied by 10%. Considering that the bridge analyses were carried out by separate users with different computer analysis programs, using different soil spring models, the results are similar, helping to validate both bridge analyses.

Bridge Retrofit Analytical Findings

Based upon the observed bridge analytical responses to eight earthquake ground motions, several retrofit methods were implemented. The object of any retrofit scheme is to increase the capacity of the bridge and/or decrease the demand on the bridge. Reducing the displacement demands was the goal of the retrofit schemes in this research, to reduce the column and expansion joint damage that was predicted to occur under the large earthquake ground motions. For the retrofit study, friction dampers, viscous dampers and transverse link beams were used to

improve the bridge seismic performance.

The bridge axes that saw the largest demand determined the orientation of the friction dampers in the bridge models. For bridge 5/826, the longitudinal direction of the bridge experienced a greater demand, while the transverse axis controlled for bridges 5/518 and 5/227. Arrangement of the friction dampers was limited to a scheme that did not impede the flow of traffic. The friction damper layout scheme used for bridges 5/518 and 5/227 are shown in Figure 33a. It consisted of adding two diagonal friction dampers at each bent running from the top of the center column to the bottom of the outer columns. This layout scheme investigated reducing the demand in the transverse axis. The friction damper layout scheme for bridge 5/826 is shown in figure 34a. This layout scheme was aimed at reducing transverse and longitudinal displacement demand in the bridge. At the center bent, there were two diagonal friction dampers running from the top of the center column to the bottom of the outer columns. Because of the skewed bents, the west and east bent outer columns had friction dampers angled at 45 degrees from the horizontal, oriented in line the with longitudinal axis of the bridge. For all bridges, the axial stiffness of the friction dampers was based on the largest available steel HSS member. The friction damper slip forces were varied for each damper layout scheme to determine the optimum slip forces. The slip forces chosen for bridges 5/518, 5/826, and 5/227 were 100 K (445 kN), 150 K (667 kN), and 30 K (133 kN), respectively.

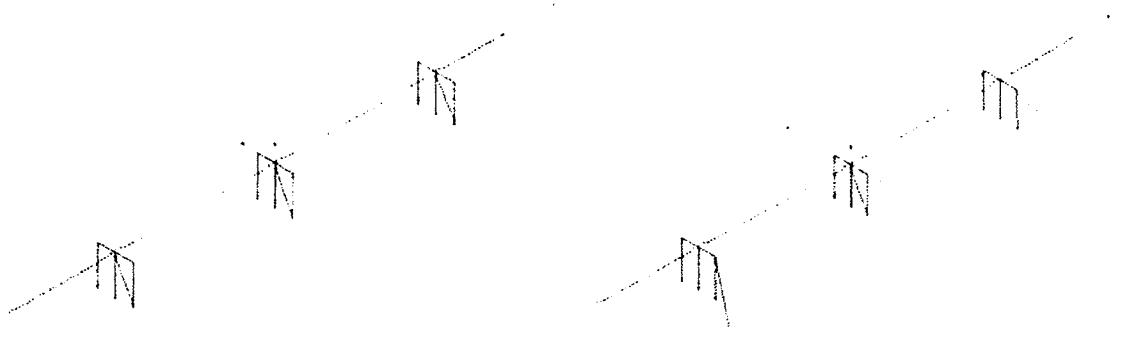

(a) (b)

Figure 33 (a) Friction Damper and (b) Viscous Damper Layouts for Bridge 5/518 and 5/227

The viscous damper layout scheme for bridges 5/518 and 5/227 are shown in Figure 31b. With this orientation of viscous dampers, the demands in the transverse and longitudinal axes of the bridges were reduced. The viscous dampers for this layout scheme were oriented so that a 45-degree angle from the vertical axis of the bridge was formed at the damper to column connection. The angle from the transverse axis of the bridge to the damper was 30 degrees. For bridge 5/826, the viscous damper layout scheme was the same as the friction damper retrofit. In all bridge models, damping ratios were kept below 35 percent. The damping constant for the final layout schemes for bridges 5/518, 5/826, and 5/227 were 500 K-s/ft (7297 kN-s/m), 600 K-s/ft (8756 kN-s/m) and 200 K-s/ft (2919 kN-s/m), respectively.

Transverse link beams were implemented in bridges 5/518 and 5/227. Transverse link beams would not benefit bridge 5/826 as significantly as the other bridges because the longitudinal axis of bridge 5/826 experienced the largest displacement demand. Frame members located at the mid-height of the columns were used to model the link beams (see Figure 32b). The cross-sectional height and width of the link beams were 3 ft (0.91 m). The link beams were modeled as linear elastic members. Plastic hinging was forced to occur in the columns at the top, bottom, and just underneath the link beams. Because link beams add considerable stiffness to each bent, the shear demand on each column is critical to monitor.

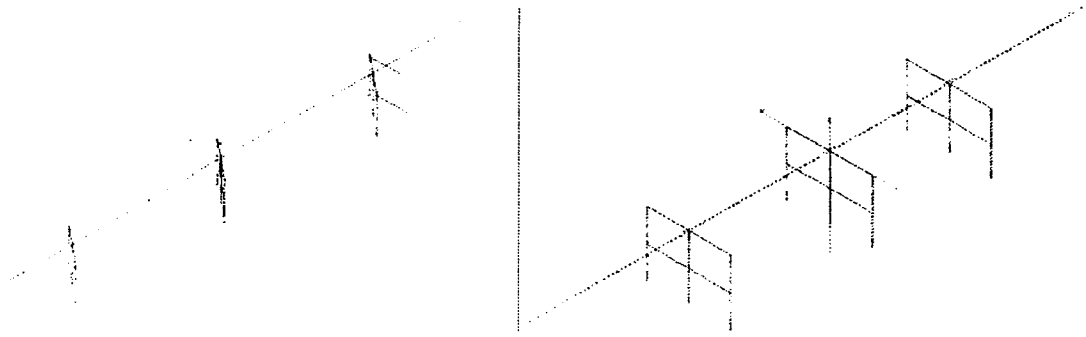

(a) (b)

Figure 34 (a) Friction and Viscous Damper Layout for Bridge 5/826 (b) Link Beam Layout for Bridge 5/227

Comparison of Retrofitting Schemes

Presented in this section are selected time-history analysis results for retrofitted bridges 5/518, 5/826 and 5/227.

Bridge 5/518 Comparison

This section discusses the bridge retrofit results for the Moquegua, Peru and Olympia, WA 975-year earthquake ground motions with soil spring stiffnesses based on E_s = 1000 ksf (47.9 MPa) and E_s = 18000 ksf (861.8 MPa). The percent change in the maximum displacements, shear forces, and moments at the center bent for each retrofit method is shown in Table 11. It can be seen that for all earthquake ground motions and soil values, each retrofit method reduced transverse and longitudinal displacements at all bents. In addition, for all analyses, the viscous dampers consistently had the largest effect in decreasing the maximum column displacements. Table 11 shows that for all analyses, the maximum transverse shear force was reduced with the friction and viscous damper retrofits, and were significantly increased for the link beam retrofit. The effect on the maximum longitudinal shear force varied depending on

the earthquake and soil spring stiffness used. For the link beam models, the maximum transverse and longitudinal column bottom moments were considerably smaller than the pre-retrofit values.

The bearing pad displacements showed several trends. For the friction dampers, viscous dampers and link beams, the abutment bearing pad displacements were reduced and the bent bearing pad displacements were increased for both earthquake ground motions and soil spring stiffness values. For the bridge models with soil spring stiffnesses based on E_s = 1000 ksf (47.9 MPa) and E_s = 18000 ksf (861.8 MPa) subjected to the Moquegua, Peru earthquake ground motions, bearing pad failure occurred at all bents for the friction dampers and link beams. For the viscous dampers, the center bent was the only bearing pad that did not fail. For the Olympia, WA earthquake ground motions (975-year return period), the only bearing pad to fail with the link beam retrofit was the west bent for soil spring stiffnesses based on E_s = 1000 ksf (47.9 MPa).

Table 11 Bridge 5/518 Maximum Reduction in Displacement, Shear and Moment Demands

Bridge 5/518		**% Reduction (-) / Increase (+) for Center Bent**							
Ground Motions & Soil Values	**Retrofit Method**	**Max. Displacement**		**Max. Shear**		**Base Moment**		**Top Moment**	
		Tran.	**Long.**	**Tran.**	**Long.**	**Tran.**	**Long.**	**Tran.**	**Long.**
Peru – Es = 1,000 Ksi (47.9 MPa)	Friction	-39	-17	-10	-1	+5	-11	-6	-7
	Viscous	-62	-28	-21	-4	+1	-22	-5	-19
	Link Beam	-34	-7	+62	-4	-64	-34	+4	-1
Peru – Es = 18,000 Ksi (861.8 MPa)	Friction	-42	-17	-11	-6	+9	-14	-7	-9
	Viscous	-62	-39	-16	-7	+9	-15	-1	-12
	Link Beam	-38	-9	+76	+16	-55	-25	+4	-16
Olympia – Es = 1,000 Ksi (47.9 MPa)	Friction	-62	-8	-10	+53	+1	-15	-6	-13
	Viscous	-62	-14	-28	-4	-6	-29	-10	-26
	Link Beam	-35	-7	+48	+64	-39	-39	-12	-18
Olympia – Es = 18,000 Ksi (861.8 MPa)	Friction	-26	-8	-10	-12	+5	-8	+8	+11
	Viscous	-50	-21	-13	-29	-4	-14	-4	-14
	Link Beam	-32	-11	+64	-17	-31	-31	+13	-24

Bridge 5/826 Comparison

This section discusses the bridge retrofit results for the Moquegua, Peru and Mexico City, Mexico earthquake ground motions with soil spring stiffnesses based on E_s = 1000 ksf (47.9 MPa) and E_s = 18000 ksf (861.8 MPa), respectively. The link beam retrofit scheme was not studied due to the governing response in the longitudinal direction of the bridge. The percent change in the maximum displacements, shear forces, and moments at the center bent for each retrofit method is shown in Table 12. For all earthquakes and soil values, each retrofit method reduced transverse and longitudinal displacements at all bents. For all analyses, the viscous dampers consistently had the largest effect in decreasing the maximum longitudinal and transverse column displacements. For three of the four analyses the maximum shear force was increased with the friction damper retrofit. For all analyses the viscous damper retrofits reduced the maximum shear force. For all soil spring stiffness values, maximum transverse moments at the center bent were reduced with the friction and viscous damper retrofits.

Table 12 Bridge 5/826 Maximum Reduction in Displacement, Shear and Moment Demands

Bridge 5/826		**% Reduction (-) / Increase (+) for Center Bent**							
Ground Motions & Soil Values	**Retrofit Method**	**Max. Displacement**		**Max. Shear**		**Base Moment**		**Top Moment**	
		Tran.	**Long.**	**Tran.**	**Long.**	**Tran.**	**Long.**	**Tran.**	**Long.**
Peru – Es = 1,000 Ksi (47.9 MPa)	Friction	-30	-47	+9	-8	-45	-25	-29	-29
	Viscous	-46	-65	-1	-14	-55	-30	-18	-28
Peru – Es = 18,000 Ksi (861.8 MPa)	Friction	-34	-46	-5	-11	-30	-16	-4	-19
	Viscous	-45	-65	-7	-12	-30	-11	-31	-17
Mexico – Es = 1,000 Ksi (47.9 MPa)	Friction	-16	-60	+6	-41	-27	-29	-39	-5
	Viscous	-44	-65	-22	-65	-65	-54	-65	-43
Mexico – Es = 18,000 Ksi (861.8 MPa)	Friction	-21	-60	+9	-21	-14	-19	-29	-16
	Viscous	-49	-65	-14	-51	-65	-38	-65	-36

Bridge 5/227 Comparison

This section shows the results for the Moquegua, Peru and Olympia, WA earthquake ground motions with soil spring stiffnesses based on E_s = 0.24 MPa (5 ksf) and E_s = 861.8 MPa (18000 ksf). The percent change for the maximum displacements, shear forces, and moments at the center bent is shown in Table 13. For all earthquakes and soil spring stiffness values, each retrofit method reduced displacements at all bents. The viscous dampers had the largest effect in decreasing the maximum column displacement demand. The maximum transverse shear force was reduced with the friction and viscous damper retrofits, but was significantly increased for the link beam retrofit. The maximum longitudinal shear force increased in a few cases for the friction damper retrofits. The link beam retrofit also significantly increased the maximum longitudinal shear force for all analyses. For all soil spring stiffness values, maximum transverse and longitudinal moments at the column bottom for all retrofit methods were reduced from the pre-retrofitted moments. The column top maximum transverse and longitudinal moment was reduced for the friction and viscous damper retrofits. For the link beam, the maximum transverse and longitudinal column top moments were larger than the pre-retrofit values.

Table 13 Bridge 5/227 Maximum Reduction in Displacement, Shear and Moment Demands

Bridge 5/227		% Reduction (-) / Increase (+) for Center Bent							
Ground Motions & Soil Values	Retrofit Method	Max. Displacement		Max. Shear		Base Moment		Top Moment	
		Tran.	Long.	Tran.	Long.	Tran.	Long.	Tran.	Long.
Peru – Es = 5 Ksi (0.24 MPa)	Friction	-55	-14	-28	+1	-8	-36	-9	-47
	Viscous	-57	-38	-32	-8	-11	-48	-11	-50
	Link Beam	-80	-52	+153	+17	-74	-20	+16	+14
Peru – Es = 18,000 Ksi (861.8 MPa)	Friction	-64	-30	-27	+15	-16	-46	-14	-49
	Viscous	-57	-26	-24	0	-17	-49	-13	-52
	Link Beam	-86	-64	+153	+46	-65	-22	+24	+11
Olympia – Es = 5 Ksi (0.24 MPa	Friction	-79	-26	-32	+30	-27	-48	-21	-36
	Viscous	-57	-53	-34	-1	-24	-57	-20	-47
	Link Beam	-85	-33	+86	+82	-69	-39	+24	+6
Olympia – Es = 18,000 Ksi (861.8 MPa)	Friction	-74	-18	-22	+7	-2	-38	-7	-55
	Viscous	-57	-36	-32	-8	-11	-41	-12	-58
	Link Beam	-72	-25	+160	+63	-63	-29	+41	+10

Based on the performance of the retrofit techniques, the most efficient retrofit method for all three bridges was the viscous damper. The viscous dampers reduced column displacements, along with column shear forces. With viscous dampers the bridges performed well in the Moquegua, Peru, Olympia, WA and the Mexico City, Mexico earthquakes. However, bearing pad failure was still predicted in all three earthquakes. The thesis "Seismic Assessment and Retrofit of Existing Multi-Column Bent Bridges" (Cox, 2005) can be referenced for more detailed information on the bridge retrofit modeling and analysis.

Conclusions

Three typical pre-1975 WSDOT pre-stressed concrete multi-column bent bridges were chosen for seismic evaluation and retrofit assessment. Most of the seismically deficient single column bent bridges in western Washington have been upgraded seismically. However, with limited funding to improve thousands of multi-column bent bridges, a prioritization of these bridges is necessary. Eight earthquake ground motions were used for nonlinear time history analysis of the bridges: three 475-year return period ground motions (Mexico City, Mexico, 1985; Kobe , Japan, 1995; and Olympia, Washington, 1949) with peak ground accelerations (PGA's) of approximately 0.3g and spectral accelerations of approximately 0.7g for a structural period of 0.5 seconds ($S_{A(T=0.5s)}$; the three bridge fundamental periods ranged from 0.4-0.6 seconds); three 975-year return period ground motions (Mexico City, Mexico, 1985; Kobe , Japan, 1995; and Olympia, Washington, 1949) with PGA's of approximately 0.5g and $S_{A(T=0.5s)}$ of approximately 1.0g; and two large Cascadia Subduction-Zone (CSZ) earthquake ground motions (Moquegua, Peru, 2001; Llolleo, Chile, 1985) with PGA's of approximately 0.6g and $S_{A(T=0.5s)}$ of approximately 1.2g. These CSZ ground motion spectral accelerations are similar to the 2003 United States Geological Survey (USGS) 2475-year return period spectral acceleration values for Seattle, WA, for structural periods equal to 0.5 seconds. The 2005 Earthquake Engineering Research Institute "Scenario for a Magnitude 6.7 Earthquake on the Seattle Fault" (EERI, 2005) predicted PGA's exceeding 0.7g, larger than the CSZ ground motion PGA's used in this research. It should also be noted that the 2001 Nisqually, WA earthquake generated PGA's of approximately 0.3g (EERI, 2005). All ground motions were modified appropriately to fit target acceleration response spectra for the Seattle area.

For the three ground motion records with 475-year return periods, predicted bridge damage was limited to light cracking in the columns and minor damage to the expansion joints of all three bridges. For the four ground motion records with 975-year return periods, moderate cracking, including spalling of the cover concrete in the plastic hinge region, was predicted in the columns of all the bridges. The column force/displacement demands still did not approach the column shear capacity envelopes, however, some of the bridge deck expansion joints were severely damaged under the 975-year return period earthquakes for bridges 5/518 and 5/826, but not for bridge 5/227. The 2475-year return period ground motions resulted in a wide range of bridge damage, from moderate cracking in the column plastic hinge regions in bridge 5/826, to likely shear/lap splice failure of columns in bridges 5/518 and 5/227. Significant column damage in bridge 5/518 and 5/227 was due to light transverse confinement, small column aspect ratios, and the non-monolithic bridge decks, which contributed to large displacements in the transverse direction. The bridge deck expansion joints were also predicted to suffer damage under the 2475-year return period ground motions for bridges 5/518 and 5/826.

Column footing demand/capacity ratios were also checked for each analysis; significant damage was not predicted. If the columns were retrofitted, resulting in an increase in the column demands, the demand on the footings could exceed the capacity of the footings. Therefore, further investigation of the foundations is necessary if column retrofit is implemented. Due to failure of prestressed concrete girders in one bridge during the 2001 Nisqually, WA earthquake, the girder demand/capacity ratios were also monitored closely, however, the demands did not exceed the capacities in any of the analyses. It is likely that significant dynamic amplification (which was not assessed in this research) occurred due to pounding of the girders against the

girder stops, resulting in a torsional response of the girders, leading to large girder demands for that particular bridge.

The effects of soil-structure-interaction were investigated and found to be influential for all the bridge analyses. The soil-structure-interaction study revealed that each bridge responded uniquely to variations in soil spring stiffnesses. When soil spring stiffnesses were changed, the maximum column displacements varied for all three bridges. In addition, modeling the column footings with fixed boundary conditions and the abutments with rollers in the longitudinal direction resulted in inaccurate and often unconservative bridge seismic assessment, illustrating the need for including soil-structure-interaction to accurately model the bridge response.

The purpose of any retrofit procedure is to increase the capacity and/or reduce the demand on a structure. Bridge columns wrapped with steel or composite jackets has been proven effective for improving column displacement capacity. Reducing displacement demands without significantly increasing the shear force demands was the goal of the retrofit schemes in this research. The three retrofit techniques implemented in this research were: friction dampers, viscous dampers, and transverse link beams. The link beams proved effective in reducing column displacements, but the column shear force/displacement demand was increased past the shear capacity of the columns. A possible retrofit scheme could include constructing transverse link beams and wrapping columns with steel jackets to increase the shear capacity of the columns.

Friction dampers proved effective for all bridges. Several layout schemes were investigated. The trends in displacement reduction for the varied soil spring stiffnesses and different earthquake ground motions were similar for the three bridges. Trends in shear force demand varied for each ground motion, but the shear force/displacement demand with the

friction dampers did not exceed the column shear capacity envelopes. Analytically, the optimum retrofit method for all three bridges was the viscous damper retrofit. Viscous dampers were chosen with the criteria that less than 35% critical damping could be obtained. The retrofits with viscous dampers were effective at reducing displacement demand in the columns, and reducing the column shear force demands. However, using friction dampers for retrofit might be a more cost effective solution. A cost analysis should be performed in order to choose which retrofit scheme to use for a given bridge.

Overall, this research on the seismic response of typical pre-1975 pre-stressed concrete multi-column bent bridges in western Washington State highlighted the vulnerability of non-monolithic bridge decks and shear-dominated bridge columns in pre-1975 WSDOT prestressed concrete multi-column bent bridges as well as the need for the inclusion of soil-structure-interaction, calibrated force-displacement characterization of columns and detailed modeling of the interaction between bridge components (e.g. proper modeling of nonlinear impacting of non-monolithic decks) for accurate bridge seismic assessment. In the end, the seismic assessment of bridges is a cost/efficiency issue. Because each bridge is different, investing in improved analyses up front will enable an efficient use of the limited funds for bridge improvement.

Recommendations

Based on the results of this research, the following recommendations are made:

- Due to variation in bridge deck type, column aspect ratios, column and abutment foundation design, bridge width and span, etc...seismic assessment of prestressed concrete multi-column bent bridges requires analyzing each bridge as a multiple-degree-of-freedom system

- Inclusion of soil-structure-interaction in bridge seismic assessment is necessary, fixed column bases and abutments with roller boundary conditions lead to inaccurate results that are often unconservative; minimum foundation modeling should incorporate linear secant stiffness springs
- In order to assess bridge columns, column force/displacement hysteresis behavior should be calibrated to experimental test data and plotted versus the degrading column shear force capacity envelope
- Bridges with non-monolithic decks warrant additional analyses due to increased transverse displacement demands and multiple expansion joint interaction
- To decrease the bridge seismic displacement demand, investigation of the use of both friction and viscous dampers is warranted.

Acknowledgements

This research was conducted through the Washington State Transportation Center (TRAC) and under contract to the Washington State Department of Transportation (WSDOT). The financial support provided by WSDOT is greatly appreciated. In addition, WSDOT project coordinator Dr. Chyuan Shen Lee was very helpful with providing information on the bridges throughout the project and discussing the bridge analyses.

Resources

AASHTO. (2005). LRFD Bridge Design Specifications, 3rd Edition. American Association of State Highway and Transportation Officials.

Abrahamson, N. A. (1998). "Non-Stationary Spectral Matching Program RSPMATCH." PG&E Internal Report, University of California, Los Angeles.

Atkinson, G. M. and Boore, D. M. (2003). "Empirical Ground-Motion Relations for Subduction-Zone Earthquakes and Their Application to Cascadia and Other Regions." *Bulletin of the Seismological Society of America*, Vol. 93 No. 4, 1703-1729.

Bowles, J.E. (1995). "Foundation Analysis and Design." New York; McGraw Hill Co. 5th Ed.

Caltrans (2004). "Seismic Design Criteria" Section 1.1 and Section 7-Design. Version 1.3.

Carr, A.J. (2004). *Volume 3: User Manual For the 3-Dimensional Version, Ruaumoko3D.* University of Canterbury.

Carr, A.J. (2004). *Volume 3: User Manual For the 3-Dimensional Version, SPECTRA.* University of Canterbury.

Chai, Y.H., Priestley, M.J.N., Seible, F. (1991). "Seismic Retrofit of Circular Bridge Columns for Enhanced Flexural Performance." *ACI Structural Journal*, 88(5) 572-584.

Chang, F. K. and Krinitzsky, E. L. (1997). "Duration, spectral content, and predominant period of strong motion earthquake records from western United States," *Miscellaneous Paper 5-73-1*, U.S.A.C.E. Waterways Experiment Station, Vicksburg, Mississippi.

Cox, C. (2005). " Seismic Assessment and Retrofit of Existing Multi-Column Bent Bridges." M.S. Thesis, Department of Civil and Environmental Engineering, Washington State University.

Dobry, R., Idriss, I.M., and Ng, E. (1978). "Duration characteristics of horizontal components of strong motion earthquake records," *Bulletin of the Seismological Society of America*, 68(5), 1487 – 1520.

EERI. (2005). "Scenario for a Magnitude 6.7 Earthquake on the Seattle Fault," Earthquake Engineering Research Institute and the Washington Military Department Emergency Management Division, 2005.

Filiatrault, A. (2002). *Elements of Earthquake Engineering and Structural Dynamics*, Polytechnic International Press, Montreal Canada.

Gregor, N. J., Silva, W. J., Wong, I. G., and Youngs, R. R. (2002). "Ground-Motion Attenuation Relationships for Cascadia Subduction Zone Megathrust Earthquakes Based on a Stochastic Finite-Fault Model." *Bulletin of the Seismological Society of America*, Vol. 92 No. 5, 1923-1932.

Hanks, T. C., and McGuire, R. K. (1981). "The character of high-frequency strong ground motion," *BSSA*, 71, 2071-2095.

Jaradat, O.A. (1996). "Seismic Evaluation of Existing Bridge Columns." Ph.D. Dissertation, Department of Civil and Environmental Engineering, Washington State University.

Kuebler, S.E. (1997). "Evaluation of Seismic Retrofit Strategies for Multi-Column Bridge Bents", M.S. Thesis, Department of Civil and Environmental Engineering, Washington State University.

Lam, I., Martin, G. (1986). "Seismic Design of Highway Bridge Foundations." *Applied Technology Council*, Report No. FHWA/RD-86/102.

LPile4.0. (2000). Reese, L.C., Wang, S.T, Isenhower, W.M, Arrellaga, J.A. "LPILE PLUS" Version 4.0.

Ludwin, R. (2002). "Deep Quakes in Washington and Oregon", Pacific Northwest Seismograph Network (PNSN), University of Washington. Accessed online at: http://www.pnsn.org/INFO_GENERAL/plates.gif.

Mealy, T.E. (1997). "Seismic Performance and Retrofit of Multi-Column Bridge Bents", M.S. Thesis, Department of Civil and Environmental Engineering, Washington State University.

PanGEO Inc., (2005). "Aurora Avenue Bridge." Accessed online at: http://pangeoinc.com.

PNSN (2005). "Deep Quakes in Washington and Oregon." Pacific Northwest Seismograph Network, University of Washington. Accessed online at: <http://www.pnsn.org/INFO_GENERAL/platecontours.html>

Priestley, M.J.N., Seible, F., Calvi, G.M. (1996). *Seismic Design and Retrofit of Bridges.* New York. John Wiley & Sons.

Priestley, M.J.N. (2003). "Myths and Fallacies in Earthquake Engineering, Revisited." *The Mallet Milne Lecture*, Rose School; Pavia, Italy.

Priestley, M.J.N., Seible, F., Chai, Y.H., Sun, Z.L. (1991). "Flexural Retrofit of Bridge Columns by Steel Jacketing." *Proceedings of the First Annual Seismic Workshop*, California Department of Transportation, Division of Structures, 203-208.

Stapleton, S.E. (2004). "Performance of Poorly Confined Reinforced Concrete Columns in Long-Duration Earthquakes." M.S. Thesis, Department of Civil and Environmental Engineering, Washington State University.

Thompson, T. (2004). "The Effects of Long-Duration Earthquakes on Lightly Reinforced Concrete Bridges." M.S. Thesis, Department of Civil and Environmental Engineering, Washington State University.

USGS. (2003). "National Seismic Hazard Mapping Project." United States Geologic Survey. Accessed online at: http://eqhazmaps.usgs.gov/.

Vader, A.S. (2004). "The Influence of Signature Tower Passive Energy Dissipating Devices on the Seismic Response of Long-Span Cable-Supported Bridges." M.S. Thesis, Department of Civil and Environmental Engineering, Washington State University.

Washington State Department of Transportation (WSDOT). (2005). "Bridge Design Manual." Chapter 4.4.

Zhang, Y., Cofer, W. F., and McLean, D. I. (1999). "Analytical Evaluation of Retrofit Strategies for Multi-Column Bridges," *Journal of Bridge Engineering*, Vol. 4, No. 2, pp. 143-150.